Employing Intracranial EEG Data to Decipher Sleep Neural Dynamics

Andrew Kvavilashvili

Thesis submitted to the faculty of Virginia Polytechnic Institute and State University in partial fulfillment of the requirements for the degree of

Master of Science

In

Translational Biology, Medicine, and Health

Sujith Vijayan

Rachel Diana

Daniel English

Della Williams

December 15, 2022

Blacksburg, VA

Keywords: Sleep, sleep spindles, intracranial EEG, learning, memory

Abstract

Over the course of a typical night, sleep is comprised of multiple different stages that involve changes in brainwave patterns. Intracranial EEG (iEEG) is an invasive brain recording technique used in hospital settings in epileptic patients to determine the focus of their seizure activity. The intracranial data recorded allows one to directly observe the neural activity of deep brain structures such as the hippocampus and to detect single unit activity and local field potentials, thus providing a level of physiological detail normally available only in animal studies. In this thesis we employ intracranial data to advance our understanding of sleep neural dynamics in humans, and to this end its focus is in two areas : (1) developing a way of sleep scoring iEEG data and (2) investigating the neural dynamics of a particular waveform found during sleep, the sleep spindle, and its role in memory consolidation.

Typically, iEEG recordings do not include electrooculogram or electromyogram recordings, which are normally needed for sleep scoring—especially for scoring rapid-eye movement (REM) sleep. We identified differences in alpha power between wake and REM sleep to develop a methodological way to reliably differentiate between wake and REM sleep states.

We also wanted to investigate the neural dynamics involved with a particular brainwave seen during sleep, the sleep spindle, which is thought to be important for sleep-mediated memory consolidation. Historically, sleep spindles were thought to occur synchronously across the cortex, but recent findings using iEEG have identified that sleep spindles can also be local. We utilized intracranial EEG to confirm previous findings that iEEG can identify local sleep spindles. In addition to identifying local sleep spindles, we aimed to investigate the potential role that sleep spindles have on learning and memory using standard targeted memory reactivation paradigms for

both procedural and declarative memories. We found that local sleep spindles occurred at a specific time following auditory stimulation for both procedural and declarative memories.

This work has opened up the use of iEEG recordings to investigations of REM sleep dynamics and laid the groundwork for examining the role of local sleep spindles in memory consolidation.

General Audience Abstract

During a night of sleep, our brain goes through different stages that exhibit changes in brainwave patterns. Intracranial EEG (iEEG) is an invasive brain recording technique used in hospital settings in epileptic patients to determine the focus of their seizure activity; this particular brain recording technique allows one to observe the brain activity of deep brain structures. By using iEEG data, we aimed to (1) develop a way of sleep scoring iEEG data and (2) investigate the neural dynamics of a particular waveform found during sleep, the sleep spindle, and its role in memory consolidation.

Electrooculograms (EOG) are used to record the electrical activity of eye movements, and electromyograms (EMG) are used to measure muscle activity. Both of these recording techniques, in addition to EEG, are needed for sleep scoring, especially rapid eye movement (REM) sleep. However, typical iEEG recordings do not have EOGs and EMGs applied to the patient. Using iEEG data, we were able to identify differences in a specific brainwave, the alpha rhythm, between wakeful brain activity and REM sleep brain activity. Furthermore, we were able to use this difference to reliably score REM sleep in iEEG data without the need for EOGs and EMGs.

We also wanted to investigate the brainwave changes in a particular waveform, the sleep spindle, that has been thought to be important for sleep-mediated memory consolidation. Previous research using typical EEG recordings showed that sleep spindles occur synchronously across the cortex, but recent findings using iEEG have identified that sleep spindles can also occur asynchronously across the cortex. We replicated previous research showing that these local sleep spindles are identifiable using iEEG recordings. In addition to identifying local sleep spindles, we investigated the potential role that sleep spindles have on learning and memory. To do so, we used standard targeted memory reactivation paradigms for two types of memory: declarative and procedural memory. We found that local sleep spindles occurred at a specific time following auditory stimulation for both procedural and declarative

memories.

This work has opened up the use of iEEG recordings to investigations of REM sleep dynamics and laid the groundwork for examining the role of local sleep spindles in memory consolidation.

Table of Contents

Contents

Preface/Attribution

Kyle Q Lepage, Sparsh Jain, Mark Witcher, and Sujith Vijayan are co-authors of Chapter 2: Frontal-Temporal Alpha Dynamics and REM Identification in Intracranial EEG Data.

Chapter 1: Introduction

Sleep is a complex phenomenon that, in one form or another, is a natural part of every living creature's life.[1,2] The very first investigations into what could possibly be happening inside our heads while we sleep was done in the 1930s during the first electroencephalographic (EEG) sleep study[3-5]. This was the first study to demonstrate and characterize the different stages of non-rapid eye movement (NREM) sleep, one of the two types of sleep. The other type of sleep, rapid eye movement (REM) sleep, was not identified until roughly 20 years later.[3-6]

Despite its prevalence in everyday life, the functional role and purpose of sleep remains quite contentious in the realm of sleep science. Many decades of sleep research have sprouted numerous theories as to why we sleep including, but not limited to theories of energy conservation, theories on sleep being a restorative period for the body, and sleep playing a major role in the consolidation of memories.[3] Though these theories all have some scientific evidence to support their claims, extant literature shows a wide breadth of evidence that sleep promotes the consolidation of memories, and that a lack of sleep is a hindrance to the consolidation of memories.[1,2,7-12] While we now know that sleep plays a vital role in the consolidation of our memories, the underlying mechanisms involved in this process remain enigmatic. However, there is a lot of evidence to suggest that the unique brainwave patterns that occur during certain stages of sleep are vital for the consolidation of memories.[2,7,13,14]

The Different Stages of Sleep

Non-rapid eye movement sleep is subdivided into three stages: N1, N2, and N3 while REM sleep makes up the fourth stage; each stage is characterized by distinct patterns of brain activity.[3] First, wakeful brain activity needs to be identified in order to differentiate the brain states between wakefulness and sleep. Wakeful brain activity is characterized by anteriorly distributed beta

rhythms and posteriorly distributed alpha rhythms; these alpha waves can only be observed during relaxed wakefulness while the eyes are closed.[3,20] Additionally, wakeful activity includes eye movements and eye blinks. The brain activity in N1 sleep typically shows an absence of the previously mentioned beta and alpha rhythms and, instead, globally distributed low-amplitude theta rhythms (4-7Hz) while eye movements slow to a "rolling" activity.[3,20] Stage N2 sleep is primarily characterized by K-complexes, a distinct waveform that begins with a negative deflection in activity that is immediately followed by a positive deflection, and sleep spindles, a waveform that lasts around 0.5 – 2 seconds with a frequency of around 11 – 16Hz.[3,5,18,19,20-23] Moving on to N3, we see brain activity drastically change to waveforms of high amplitude and a low frequency of around 0.5 – 2 Hz. Due to the slow nature of these brain waves in N3, it is aptly referred to as slow wave sleep (SWS). It is important to note that sleep spindles can be observed throughout SWS.[3,20] Last but not least, REM sleep is characterized by conjugate, irregular eye movements with brain activity that almost mimics wakeful activity. What differentiates REM sleep from wakefulness is a reduction in muscle tone.[3,20] Because of these factors, EMG and EOG, in conjunction with EEG recordings, are a necessity for proper scoring of REM sleep. While these four stages happen throughout a period of sleep, these changes in brain activity are thought to play a role in the consolidation of memories.[11,12-14,17,22]

Though standard EEG is the primary way to record the brain activity of sleep in individuals, intracranial EEG (iEEG), data exists in a plethora of hospital settings.[15,16] With the utilization of iEEG recordings, which are electrodes invasively implanted directly into the brain as opposed to the surface of the scalp as a way for pharmacologically-resistant epilepsy patients to receive treatment, we can gain further insight into the neural dynamics of sleep not available through standard EEG recording. For example, iEEG recordings are able to provide direct recordings from

deep brain structures like the hippocampus, a brain structure most notable for its role in memory.[16] Additionally, iEEG allows for the observation of brain wave patterns such as local spindles and local slow waves, which are not picked up by typical scalp EEG.[19] These unique advantages of iEEG make it useful for examining sleep dynamics, and by taking advantage of iEEG data, the goal of this thesis is twofold:

1. To develop a methodological way of sleep scoring REM sleep data from iEEG recordings. Currently, there exists a plethora of iEEG data recordings that are publicly available for research purposes, but without the inclusion of EOG and EMG electrodes, these data sets cannot be investigated for REM sleep research. By developing a way to sleep score iEEG data without the use of EMG or EOG electrodes, we will be able to make data from REM sleep more available for analysis purposes.
2. To investigate the neural dynamics of local versus global spindles during sleep. Research on sleep spindles have shown that sleep spindles play a role in memory consolidation. However, the role between local spindles and global spindles is still not well known. Local spindles can only be identified by using iEEG recordings and, currently, the functional significance of local spindles remains unanswered. To further our understanding of the significance of local spindles, and their relationship with global spindles, we will investigate sleep spindle dynamics and their effects on memory consolidation.

Chapter 2: Frontal-Temporal Alpha Dynamics and REM Identification in Intracranial EEG Data

Abstract

A large number of human intracranial EEG (iEEG) recordings, including during sleep, have been collected for clinical purposes in institutions all over the world, but the vast majority of these are unaccompanied by EOG and EMG recordings. In order to make full use of these extremely valuable data sets, an accurate method of classifying sleep from iEEG recordings alone is required; standard, broadly accepted methods of fully scoring sleep require the use of EMG and EOG recordings. Existing methods of sleep scoring using only iEEG recordings accurately classify all stages of sleep with the exception that wake (W) and rapid-eye movement (REM) sleep are not well distinguished; note that iEEG is rarely recorded occipitally.

Data were collected from nine patients (6 females and 3 males) between the ages of 19 and 55 years (mean 33.11 ± 13.99 (SD) years) undergoing invasive monitoring using intracranial depth electrodes for intractable epilepsy. Data (including EOG and EMG recordings) were scored for sleep by experienced sleep scorers and then analyzed for differences in average alpha power using multitaper spectral analysis. For the purpose of sleep scoring without EMG or EOG recordings, K-means clustering was modified for use with multivariate, multitaper spectral statistics.

Average alpha rhythm power from temporal and frontal areas in intracranial EEG recordings was shown to be greater during awake periods than during REM sleep. Among the eight subjects exhibiting normal sleep architecture, the introduced multitaper K-means sleep-scoring algorithm identified a mean duration of REM sleep equal to 36 ± 6 minutes and identified 60 and 62.5 minutes of REM sleep in the two best performing subjects.

Our novel statistical methodology is sufficient to reliably distinguish useful durations of REM sleep from Wake periods in recorded intracranial alpha activity in a population of nine subjects.

Introduction

Alpha (8-12 Hz) oscillations occur during eyes-closed wakefulness in humans but dissipate once the subject falls asleep.[43-46] This pattern of alpha activity is often used for the purpose of sleep scoring EEG data[47,48], and especially to distinguish awake periods from periods of rapid eye movement (REM) sleep, since the neural activity exhibited in EEG recordings during Wake and REM periods are otherwise similar.[2,49-52]

The alpha oscillations described above, as detected using standard EEG, are most prominent over the occipital cortex. However, intracranial patients rarely have electrodes in the occipital regions; instead, intracranial electrodes are commonly located in the temporal and frontal regions of the brain.

In our present work, we investigate whether alpha power dynamics in iEEG recordings differ across states of arousal in non-occipital areas of the brain. We then explore whether our findings can be used to distinguish Wake and REM states when relying on iEEG data only. Traditional sleep scoring mechanisms rely on the use of facial electrodes to track eye movements (electrooculography, or EOG) and muscle tone (electromyography, or EMG) to assign a sleep stage to a given epoch of EEG data. EOG and EMG electrodes are especially useful for distinguishing REM sleep from the awake state; there are published methods for determining NREM sleep periods using intracranial data alone, for example by tracking power in frequencies, such as the delta band (1-4 Hz), that characterize NREM sleep[53]. There are many intracranial EEG recordings during sleep available throughout the world but without corresponding EOG and EMG data. Thus, our motivation in this second step is to render these datasets useful by determining a method for correctly identifying periods of REM sleep based upon alpha dynamics alone. Note that for this purpose, we need not achieve an exhaustive identification of all REM sleep periods;

the ability to reliably identify even a subset opens up this invaluable data to the scientific community for the investigation of neural dynamics during REM sleep.

Materials and Methods

Data Collection

Data were collected from nine patients (6 females and 3 males) between the age of 19 and 55 years (mean 33.11 ± 13.99 (SD) years) undergoing invasive monitoring using intracranial depth electrodes for intractable epilepsy (see Table 1). Patients signed the informed consent approved by the Institutional Review Board (IRB) at Carilion Roanoke Memorial Hospital prior to participating in the study. Two to sixteen Ad-Tech depth electrodes, each with 6 to 14 macro contacts, were implanted in each subject. Note that the macro contacts are the recording points along the shaft of each electrode and are regularly spaced. Therefore, some macro contacts are located closer to the surface of the brain. The placement of electrodes was determined strictly by clinical criteria without considering research needs (See Table 2).

Electrophysiological readings from the Ad-Tech electrodes were received by a 256-channel ATLAS digital acquisition system from Neuralynx (Bozeman, MT), which was connected to a PC running Pegasus Acquisition Software from Neuralynx. The input signals were sampled at 2000 Hz. For each subject, recording started between 8 PM and midnight, depending on an estimated bedtime. EEG data from the raw Neuralynx files were converted to EDF files in blocks of 4-hour periods. For each subject, between 6 to 12 hours of sleep/wake data were recorded and considered for analysis.

Electrode Localization

The locations of depth electrode contacts were determined using Freesurfer[36,37] and IELU[38] software in two steps: reconstruction and coregistration. First, a preoperative high-resolution magnetic resonance imaging (MRI) scan was used to generate a 3D rendering of the subject's brain using FreeSurfer; this rendering was placed in a 3D coordinate system (RAS). During the reconstruction process, FreeSurfer also automatically generates subcortical and cortical parcellations with anatomical labels using the Desikan-Killiany Atlas[39]. Second, the postoperative CT scan was coregistered with the 3D rendering using the IELU pipeline, thus providing a RAS coordinate for each electrode contact. Using the FreeSurfer-generated parcellations and the RAS coordinates, we determined the anatomical location of each electrode contact with the help of a MATLAB script[40]. A quality check on localization accuracy was performed via visual inspection.

Sleep Staging

For manual sleep scoring, EEG signals from a centrally located subdermal strip and from intracranial electrodes (iEEG), electromyography (EMG), and electrooculography (EOG) were used to score sleep independently by two experienced sleep scorers using criteria specified by the American Association of Sleep Medicine for sleep.[47] All these data streams (iEEG, EMG, EOG) were simultaneously recorded using the ATLAS system and therefore synchronized. Periods identified as REM sleep were further verified by two additional sleep scorers. We note that of the subjects we examined, only subject 7 displayed unusual electrophysiological characteristics. Though epochs for subject 7 labeled as NREM or REM had many features of these respective sleep stages, all sleep stages displayed activity unusual for their respective stages as well. For instance, during REM epochs, there was often an intrusion of high voltage, low frequency activity (not slow enough to be N3) appearing on a subset of the channels, which was not typical for any

other subjects, and these intrusions occurred during periods of low EMG tone and conjugate eye movements. We marked an epoch as the beginning of a REM period only if we observed low amplitude mixed frequency activity with rapid eye movements and low chin EMG tone. However, in subject 7, some channels exhibited atypical, intermittent activity, while others exhibited typical REM activity. We included this subject for completeness and for illustrative purposes.

Data Analysis

For each subject, we identified at least one seizure-free night of sleep where the subject entered both NREM and REM sleep. As mentioned previously, most intracranial EEG subjects are implanted with frontal and temporal electrodes. We restricted our analysis to depth electrodes in these regions and to contacts near the neocortical surface, which are more likely to be seizure-free. These restrictions allow for our methods to be easily transferred to data sets collected at other centers and could allow for generalization to electrocorticography (ECoG), which records activity at the surface level of the brain. Note that contacts residing in or near the cortical regions are most likely to exhibit the neural signatures and power variations observed in standard EEG recordings for sleep studies.

Electrode and Contact Montage

From each depth electrode set, one or two outermost channels residing in the brain were initially chosen and checked against the exclusion criteria. Electrode contacts that were identified to be in the epileptic focus or identified as displaying interictal activity by the epileptologists were excluded from all analyses. In this fashion, a montage was created of temporal and frontal electrode contacts residing in, or closest to, the cortical gray matter regions (see Tables 2 and 3 showing the information for each subject). Note that each of the electrodes listed in Table 2 had 6 to 10 contacts along its shaft, and therefore some contacts were closer to the surface and some deeper in the brain.

Table 3 lists the number of contacts (all close to the surface of the brain) that were actually used for analysis in each of the brain regions. All the analyses presented here were performed using a unipolar montage with the reference being a subdermal electrode placed toward the front of the head (approximately at the location of Fz).

Data Preprocessing

First, EEG data from the selected unipolar montage of channels were filtered to remove 60 Hz and harmonic frequencies (zero-phase FIR notch filter) to suppress the noise introduced due to power line interference. Next, data was separated into non-overlapping 30-second sections, corresponding to the scored sleep stages.

Multitaper Alpha Rhythm Calculations

From each 30-second data section, 5 segments, each of 6 seconds duration, were further separated and their sample averages removed across-time. Each of these 6-second duration segments were then multiplied by the 22 lowest-order discrete-prolate spheroidal sequences. The resulting 110 tapered data sequences were then each discrete-time Fourier transformed and evaluated at 10 Hz. This process yielded 110 values characterizing the alpha rhythm for each of the iEEG channels for each sleep stage. For theoretical reasons, these 110 complex-valued quantities are known as multitaper eigencoefficients.[59] The number of tapers and segment duration were chosen to minimize spectral leakage and to characterize the frequency interval (8-12 Hz). Because the dimension of a process is approximately $2NW$[60], and there are $2NW-2$ asymptotically independent multitaper eigencoefficients, in this work, the multitaper eigencoefficients evaluated at 10 Hz are used to characterize the interval 8 Hz to 12 Hz.[43] This property is related to the special nature of the discrete prolate spheroidal data taper.[61] The multitaper method of spectral analysis is a popular method of assessing rhythms in neural data.[62,63]

Multitaper Alpha Power Estimates

For each sleep stage, alpha power was estimated by computing the sample average of the square magnitudes of the multitaper eigencoefficients (110 per 30-second episode per electrodecontact).

Per-Subject Alpha Power Comparison: Wake vs REM

For each subject, alpha power was compared between the Wake (W) and REM (R) sleep stages using two hypothesis tests.

1. A two-sample, one-sided (W > R), unpaired t-test was performed assuming unequal variances for the multitaper alpha power estimates associated with W and R epochs; an unpaired t-test was used as there is no natural pairing for Wake and REM episodes. To account for multiple comparisons, p-values were Bonferroni corrected.

2. A semi-parametric test was performed as follows. 1000 sets of surrogate data were created. Each two-group data set consisted of equal numbers of Wake (W) and REM (R) power values, populated by drawing with replacement from all the alpha power estimates computed for the subject (i.e., from the pool of estimates computed for both the R and W sleep stages). The specific group size was equal to the minimum of the number of actual Wake and REM sleep stages. For each surrogate data set (consisting of W and R alpha power estimates), the ratio of W to R group sample averages was computed. The null hypothesis is that the corresponding variable is equal to one (i.e., there is no difference in alpha power). This procedure yields 1000 ratios, which are compared against the actual ratio computed using the R and W epochs identified in the data. The p-value for this semiparametric test is equal to the fraction of surrogate groupings that yield an alpha power ratio statistic greater than the actual ratio computed using the actual R and W epochs identified in the data. This is a one-sided test for increased alpha power during Wake relative to

alpha power during REM. This test was repeated twenty times to account for the sub-selection of the Wake alpha power statistics, since for all but one of the subjects, the number of Wake sleep stages was substantially larger than the number of REM sleep stages.

Sleep Scoring Without EMG & Without EOG: Label Assignment

To assign REM and Wake labels without using the EMG or EOG recordings, the 30-second episodes, as characterized by the multitaper eigencoefficients, were clustered using a modified K-means clustering algorithm. The technical details of this modification are presented in the Appendix: Multitaper K-Means Clustering. The number of clusters used was selected as the number of clusters, among clusterings of size 1 through 14, that minimized an approximation of the Akaike Information Criterion (AIC). This approximation is discussed in Appendix: Multitaper K-Means Clustering. To assign the REM label to an epoch, the cluster tending to exhibit the lowest alpha power was identified. Specifically, for each electrode contact, clusters were ranked according to alpha power. A rank of one indicated that the average alpha power of the sleep epochs belonging to that cluster was at a minimum (over all cluster alpha powers), for that electrode contact. For each cluster, the median of these rankings was computed across electrode contacts. The epochs belonging to the cluster with the lowest median ranking (referred to as the REM cluster for the remainder of this paper) were assigned the REM sleep stage label.

Sleep Scoring Without EMG & Without EOG: Step-by-Step Procedure

The following procedure was used to distinguish between REM and Wake episodes: 1) iEEG data was recorded. 2) The data was sectioned into 30-second stages. 3) NREM stages were removed using published methods that rely on spectral features of NREM sleep such as delta power.[53] 4) Each of the remaining stages was subdivided into 5 sections, each 6 seconds in duration. For each 6-second section, 2NW-2 eigencoefficients were computed (i.e., 22) via the discrete-time Fourier

transform of the tapered 6-second duration using the corresponding discrete prolate spheroidal sequence. 5) For each 30-second sleep stage, the $N_{contacts}$ x 5 x 22 eigencoefficients were combined into one feature vector characterizing the 30-second episode. Here $N_{contacts}$ is the total number of electrode contacts used for a given subject. 6) All the feature vectors, one for each 30-second episode, were clustered using the modified K-means clustering procedure introduced in this work (see Appendix: Multitaper K-Means Clustering). 7) The minimum alpha-power cluster was identified using the procedure specified in Section labeled Sleep Scoring Without EMG & Without EOG: Label Assignment. 8) All sleep stages with feature vectors assigned to the minimum alpha-power cluster were assigned the REM sleep stage label.

Sleep Scoring Without EMG & Without EOG: Assessment of Label Confidence

We investigated a few different measures of REM label accuracy and cluster fidelity. The alpha power difference between the rank 2 and rank 1 clusters was calculated for each electrode contact, and the minimum alpha power differences (over all electrode contacts) was identified (see Table 4, fourth row). Sample size was low; however, the minimum alpha power difference correlated with REM label accuracy among the two worst-performing subjects (n = 2). REM label accuracy was computed as the fraction of REM-labeled sleep stages that were correctly labeled (Table 4, second row). Note that this statistic does not reflect the number of actual REM sleep stages that were not labeled by our scoring procedure. To assess the completeness of our REM versus Wake sleep scoring method, the fraction of all REM episodes that were correctly labeled as REM by our procedure was reported (Table 4, third row).

Results

REM vs. AWAKE Alpha Power

Across all channels, alpha power was observed to drop during periods that were marked as REM by our scoring experts versus periods marked as Wake. The spectrogram in Figure 1 illustrates the drop in power in the alpha band (8-12 Hz) during REM, as seen in Subject 6. Specifically, alpha power was lower during REM epochs than during W epochs; this pattern was observed in individual channels as well as in the average alpha trace. Figure 2 illustrates the change in alpha power over the course of the night in conjunction with a hypnogram; note the greater alpha power during awake periods than during REM sleep. This observation was examined statistically in the next step, using 2 different approaches: a t-test and a semiparametric test (see Methods). Figure 3 illustrates the distribution of W and REM epochs across the subjects. Typically, the number of Wake stages is greater than the number of REM stages. Because patients are continuously monitored in the hospital, there is no "lights out" and the time the patient goes to sleep varies. As a result, we have a fair number of recordings from W prior to sleep. In addition, patients awake during the night due to a doctor or nurse visiting the patient's room; an increase in wake time in intracranial subjects has been observed in multiple intracranial sleep studies.[64-67] Two-sample, one-sided (W > R), unpaired t-tests showed that there was significantly greater alpha power during W than during REM in all subjects except subject 7 (see Figure 4). Bonferroni-corrected p-values for all subjects except subject 7 were less than or equal to $3x10^{-9}$. These t-test results were consistent with results from the semi-parametric test for greater alpha power during Wake than during REM: all the semi-parametric test p-values were equal to zero, except for the p-value associated with subject 7. For subject 7, the hypothesis test p-value was equal to one; as mentioned in the Sleep Staging section of the Methods, subject 7 exhibited sleep abnormalities.

We repeated this analysis for all the common brain rhythms (i.e., delta, theta, beta, and gamma), and found that only alpha activity was significantly greater in Wake than in REM for all subjects exhibiting normal sleep (i.e., all except subject 7). Note that alpha activity was sufficient for our purposes—we sought only to find a quantity that would allow us to identify REM episodes, and therefore it was not necessary to consider the dynamics of other rhythms.

Identifying REM Episodes Using iEEG Alpha Power

We first wanted to get a sense of how well we could distinguish REM from W using an alpha power threshold. To do this, we calculated the empirical probability density functions of the alpha power for both REM and Wake epochs. The empirical probability density functions for REM and Wake epochs for subject 3 are shown in Figure 5A. As can be seen, there was significant overlap between the probability density functions—indicating it would be difficult to identify REM episodes based only on an alpha power threshold (see below for comparison of threshold method to our proposed method).

To achieve our desired goal of identifying REM epochs solely using iEEG data, we turned to a modified K-means method as described in the Methods (in particular, the sections Sleep Scoring Without EMG & Without EOG: Label Assignment and Sleep Scoring Without EMG & Without EOG: Step-by-Step Procedure) and in the Appendix: Multitaper K-Means Clustering. Instead of determining the sleep stage based on a threshold of average alpha power across electrodes, the clustering method uses the pattern of alpha activity exhibited by all electrode contacts to distinguish between clusters of stereotypical activity. It makes use of the alpha power on each electrode as well as the average timing relationship (over 30-second intervals) for alpha activity between the electrodes. Additionally, the clustering allows for the separation of difficult-to-distinguish stages into their own cluster, which can facilitate identifying reliable REM sleep stages.

As can be seen in Table 4, REM episodes were reliably classified by our method. By estimating the REM and Wake average alpha-power empirical probability densities using the human-labeled stages, we could assess the expected performance of a binary hypothesis test based upon average alpha power. Using the clustering procedure, we achieved high accuracy (Table 4, row 2) even for subjects with relatively high overlap in their average alpha power REM and Wake empirical probability densities.

As an example, in Figure 5A, the REM and Wake empirical probability density functions (PDFs) for subject 3 exhibited substantial overlap. As a consequence, any choice for an alpha-power binary hypothesis test threshold yielded poor results for this subject. To directly compare a binary hypothesis test based upon average alpha power with the proposed multitaper K-means clustering procedure, we specifed the average alpha-power threshold such that both the binary hypothesis test and the proposed procedure, correctly identified the same number of REM episodes.[1] For Subject 3, the proposed method made no errors while labeling 60.4% of all REM episodes (size is equal to zero). In Figure 5A, the corresponding alpha-power threshold required for the alpha-power test to label 60.4% of REM episodes is specified by the black vertical line. Using this threshold to classify episodes as REM, the number of Wake episodes specified as REM was equal to 7 (i.e., 7 Wake episodes exhibited average alpha power less than the threshold). The size of this alpha power test is 0.19 (i.e., there were 7 Type I errors out of a total of 36 tests). The proposed clustering-based classifier (see Sections in Methods labeled Sleep Scoring Without EMG & Without EOG: Label Assignment and Sleep Scoring Without EMG & Without EOG: Step-by-Step Procedure, and Appendix: Multitaper K-Means Clustering) did not specify any Wake episodes as REM for subject 3 (see Table 4, row 2). This comparison was performed for all subjects, with the proposed

method performing just as well or better than ~~out-~~ the alpha-power test in 6 of 8 subjects (excluding subject 7) and only slightly worse for the other two subjects (see Figure 5B).

As noted in the methods, the minimum alpha power difference between electrodes in rank 1 and rank 2 clusters was correlated with REM label accuracy in the two worst-performing subjects (n = 2); see the fourth row in Table 4. Excluding these two subjects raises our accuracy to 86% or better. Therefore, this metric may prove to be of use in assessing confidence in the epochs labeled as REM.

Using our method, we identified about an hour's worth of REM sleep in two of our subjects, and on average 36 ± 6 minutes of REM sleep; see first row in Table 4. In subjects without the necessary facial electrodes, these valuable REM data would not otherwise be available to researchers.

Discussion

To the best of our knowledge, this is the first study to show that alpha power, as recorded in iEEG data, is significantly greater on average during awake conditions than during REM sleep in temporal and frontal brain regions. Leveraging this observation, we also introduced a method that identifies REM epochs in data sets that otherwise would not be able to be reliably scored for REM sleep, thus making these data available to the sleep and neuroscience communities for analysis and exploration of REM neural dynamics.

Alpha Power Differences

Of the eight subjects exhibiting healthy sleep architecture, all exhibited elevated intracranial EEG alpha rhythm power during awake periods as compared with REM sleep (see Figure 4); as mentioned before, subject 7 displayed many unusual electrophysiological features during REM and NREM sleep stages. This result generalizes findings in surface EEG recordings [27,28] to the

intracranial EEG setting. We note that there were hints of this difference in other intracranial studies [29,30], but none directly examined the difference in alpha power between REM and awake conditions. This work adds to our small but growing understanding of oscillatory activity during REM sleep gained using human intracranial data [23,24,31–35]. These efforts are of importance as the details of the neural dynamics that occur during REM sleep remain much less well understood than those of NREM sleep [7,26,33,36–47]; progress here may be critical to gaining insight into how REM sleep serves its putative functions. More broadly, our findings add to the body of work showing that alpha activity is an important component of neural dynamics across multiple brain regions [48–50] and across cognitive [51–56] and arousal states[57] rather than just being associated with the visual domain when eyes are closed [58]. As mentioned, none of the other well-known brain rhythms displayed a difference in power between REM sleep and awake periods in subjects with normal sleep. We note that regardless of the dynamics of other power bands across states of arousal, the alpha rhythm dynamics are sufficient for our purposes.

Method of Identifying REM Episodes

We implemented a method for REM sleep scoring that does not employ EOG and EMG recordings to separate REM from Wake sleep stages, and that identifies REM sleep stages with accuracies greater than or equal to 73% (when analysis was restricted to the eight subjects exhibiting normal sleep architecture; see Table 4, row 2). Accuracies were greater than 86% when removing subjects on the grounds of a low minimum difference in alpha power (Table 4, row 4) between the closest competing cluster and the "REM" cluster (two subjects removed, seven remained). Note that this latter statistic also rejected subject 7 (the subject exhibiting abnormal sleep architecture) from the analysis. The relationship between alpha power difference in the competing clusters and the fraction of correctly identified REM episodes suggests that this fraction could be a means of

determining confidence level in the accuracy of identification of REM epochs. Subject 7 not only illustrates that the alpha power differences between REM sleep and awake conditions may be altered in individuals, but also gives us confidence that our clustering method is indeed leveraging this difference in a reasonable way. It is important to note that agreement among human sleep scorers has been estimated to be as low as eighty-two percent [59], an accuracy that is exceeded by the proposed method for seven of the eight subjects exhibiting normal sleep architecture.

The REM labels produced by the proposed clustering method are reliable; however, they are not exhaustive. That is, REM episodes can also be found in other clusters. For the subjects with normal sleep, i.e., all subjects except subject 7, our method selected on average 59% of all the manually sleep-scored REM episodes; our method picked out approximately 77%, 42%, 60%, 40%, 88%, 78%, 79%, and 67% of the sleep-scored REM episodes for subjects 1, 2, 3, 4, 5, 6, 8, and 9, respectively (see Table 4, row 3). For these subjects, our REM labeling accounted for 47.5, 26.0, 14.5, 22.5, 31.5, 62.5, 25.0, and 59.5 minutes of REM sleep, respectively. This method paves the way to reliably identifying REM periods from large existing intracranial data sets that lack EOG and EMG data, facilitating the use of otherwise unavailable sleep data.

Nonstandard Binary Hypothesis Test

Our procedure for identifying REM episodes is a non-standard binary hypothesis test. We labelled an episode REM, or we did not assign a label at all, and then we assessed our procedure based upon what fraction of the identified REM episodes were actually Wake episodes. This was consistent with our overarching goal of making REM periods accessible to researchers for analysis. The probability of Type I and Type II errors for our procedure are more fully discussed in Appendix: Classical Type I & Type II Testing Errors.

Conclusion

We examined intracranial data from frontal and temporal regions (which tend to be monitored in epileptic patients) to determine if there were differences in oscillatory power that might distinguish REM from awake periods. Indeed, we found that on average, alpha power is greater during awake periods than during REM sleep in these regions. We leveraged our findings regarding alpha power, using a novel clustering method, to reliably identify periods of REM sleep in human intracranial recordings without the use of EOG or EMG data. This work opens up a large number of intracranial data sets to investigations on REM sleep.

Appendix: Multitaper K-MeansClustering

The standard K-means clustering algorithm is adjusted in the following way. First, it is adjusted to include the Mahalanobis distance, such as in Cerioli (2005) and Martino et al. (2019).[101,102] Second, this distance is replaced with the full circularly-symmetric multivariate normal probability density function appropriate for a random vector with realizations in $\mathbb{C}^n$, where n is the number of electrode contacts. Here, circular symmetry means that both the real part and the imaginary part are identically distributed. They are further assumed to be mean-zero and to possess the same covariance matrix, R; this latter matrix is proportional to the cross-spectral matrix, which is Hermitian and has the electrode alpha power along its diagonal[2]. Here, $\mathbb{C}$ is the set of complex-valued numbers, each element of which possesses both a real number component and an imaginary number component.

The steps in the modified K-means algorithm are as follows:

1. Specify the number of clusters.
2. The initial observation labels are randomly guessed (as recommended in Faber (1994)[103]), and the cluster-specific covariance matrix, R, is estimated for each cluster.
3. Given the new specification of the cluster parameters, the 30-second episodes (i.e. observations) are re-clustered by assigning them the label of the cluster-specific probability density function with the largest probability density.
4. The cluster-specific covariance matrices, R, are re-computed.

[2] This model is consistent with a weak-sense stationary process model of the iEEG recordings. As a consequence, a statistically equivalent procedure could be developed based upon the electrode-contact cross-spectral densities. The approach taken here is chosen out of convenience, and allows incorporating alpha-activity cross-electrode dependence (i.e. cross-electrode alpha activity timing) within the K-means clustering procedure.

5. Steps 3 & 4 are repeated until an iteration occurs without a resulting change in observation label. Once this occurs, subsequent iterations result in no change and the algorithm has converged.

Note that this iterative procedure is a variation on standard K-means clustering and is similar to the K-means clustering algorithms discussed in Cerioli (2005), Martino et al., (2019), and Faber (1994).[101-103] For our data, by iteration 25, no changes to the stage labels occur between one iteration and the next. Upon convergence, the Akaike information criterion (AIC) for this clustering is approximated by $\tilde{AIC}$, which is equal to[3]

$$\tilde{AIC} = -2\ell(\check{\Theta}) + 2x(\textit{Number of Parameters})$$

Here, $\check{\Theta}$ is our estimate of the set-valued parameter containing the covariance R for each cluster as well as the sleep stage labels. The quantity $\ell(\check{\Theta})$ is the natural logarithm of the joint probability density function evaluated at $\check{\Theta}$. Smaller values of AIC imply a lower Kullback-Liebler divergence between the unknown data generating probability density function, and the modeled generating probability density function.[104,105] Minimizing $\tilde{AIC}$ promotes quality of fit, and penalizes model complexity (that is, clusterings comprising larger numbers of clusters are penalized). Regarding the approximate AIC it is important to note that for K-means clustering the AIC does not apply, since it is accurate only asymptotically, that is, as the number of observations grows large with

[3] The approximate AIC, $\tilde{AIC}$, is equal to the AIC in the situation where there are no missing observations (i.e. supervised learning or regression, as opposed to unsupervised learning, or clustering), the iEEG time-series are weak-sense stationary, mean-zero, and 30 seconds of recording is a sufficient duration such that the multitaper statistics are realizations of a circularly-symmetric normal distribution. An extension of AIC exists for missing observations[106] in the situation where the expectation-maximization algorithm[107] is used. K-means clustering uses a modified expectation-maximization algorithm.

respect to the number of unknowns. In the standard clustering setup (i.e. no repeated measures), each observation is assigned a cluster label; thus, the number of unknowns, just from cluster labeling, is equal to the number of observations. In this context, asymptotic results are not reliable. Let N_e equal the number of electrodes. In the current time-series context, the number of observations per electrode contact per label is 110, and the number of parameters is equal to $(N_e^2 + N_e)/2$. In this setting, application of asymptotically valid statistics is standard practice.

Lastly, the procedure consisting of steps 1 through to 5 above produces a single clustering. In the full procedure, thirteen clusterings are computed, each one associated with a different a priori specified number of clusters. The final, selected clustering is the one that minimizes $\tilde{AIC}$ specified in Eqn. (1).[106]

Appendix: Classical Type I & Type II Testing Errors

Consider the binary classification of Wake and REM stages as a statistical binary hypothesis test. Associate REM with the null hypothesis H_o and Wake with the alternate hypothesis H_a. Let the observedfeaturevectorbeequalto **v** andthe region of feature space associated with the REMcluster be C. The Type II Error, $P(Select\ H_0 \mid H_a)$, is equal to,

$$P(Select\ H_0 \mid H_a) = P(Select\ H_0 \mid v \in C, H_a)P(v \in C \mid H_a) + P(Select\ H_0 \mid v \notin C, H_a)P(v \notin C \mid H_a) \quad (1)$$

Here $P(v \in C \mid H_a)$ is equal to the fraction of Wake episodes with feature vectors belonging to the REM-identified cluster. Similarly, $P(v \notin C \mid H_a)$is equal to the fraction of Wake episodes assigned to the

non-REM specific clusters. Continuing,

$$P(SelectH_o|H_a) = P(SelectH_o|v \in C, H_a)P(v \in C|H_a) + P(Select\ H_o|\ v \notin C, H_a)P(v \notin C\ |\ H_a)$$

$$= 1\ x\ P(v \in C|H_a) + 0\ x\ P(v \notin C|H_a)$$

$$= P(v \in C\ |\ H_a) \qquad (2)$$

That is, the probability of assigning an awake episode to REM is equal to the probability that an awake feature vector lies in C and is Wake. This value is equal to 1 minus the second row in Table 4 for each of the subjects. Now, consider the Type I error, $P(Select\ H_a|\ H_o)$. Because our procedure does not label episodes associated with $v \notin C$ (i.e. episodes belonging to the non-REM cluster), the relevant figure ofmerit that is analogous to the Type Ierror, is the modified Type Ierror, $P(Select\ H_a\ |\ v \in C, H_o)$. In this sense, our procedure is a non-standard binary hypothesis test. We label an episode REM, or we don't label it at all, and then we assess our procedure based upon what fraction of the identified REM episodes are actually Wake. The modified type I error is:

$$P(Select\ H_a|\ v \in C, H_o) = P(Select\ H_a|\ v \in C) = 0 \qquad (3)$$

All episodes associated with feature vectors in C are assigned the REM label. We further assess this labeling procedure in one other way. We ask, simply, how much REM sleep do welabel as REM? The answer is more than enough to do REM sleep studies (see the first row of Table 4).

Tables

Subject	Gender	Age	Handedness	Diagnosis	Imaging
1	F	24	R	Focal epilepsy, left and right temporal lobe	PET: Bilateral mesial temporal hypometabolism. MRI: Normal
2	F	41	R	Focal epilepsy, left temporal lobe	PET: Borderline symmetric hypometabolism involving mesial temporal lobes. MRI: Normal
3	F	55	R	Medical refractory epilepsy with bilateral hippocampal foci	PET: Minimal hypometabolism of left medial and inferior temporal lobe. MRI: Normal
4	F	52	R	Intractable epilepsy, bilateral hippocampal	PET: Hypometabolism left para-hippocampal gyrus. MRI: Bilateral Hippocampal Cyst, 1-2 mm. Infarct, superior right cerebellum.
5	M	29	R	Epilepsy of bilateral temporal origin	PET: Hypometabolism bilaterally in the medial temporal lobes. MRI: Normal
6	M	19	L	Seizures of right temporal origin	PET: Hypometabolism in the right temporal lobe relative to left temporal lobe. MRI: Normal

7	F	20	R	Refractory epilepsy, left frontotemporal	PET: Small area of non-significant hypometabolism in left mesiotemporal region. MRI: Normal
8	M	38	R	Medically intractable epilepsy, left hemisphere	PET: Subtle hypometabolism predominantly in right parietal lobe. MRI: Normal
9	F	20	R	Medical refractory epilepsy with bilateral hippocampal foci	PET: Minimal hypometabolism of right lateral temporal lobe. MRI: Unremarkable (incidental finding of bilateral hippocampal cysts)

Table 1: Patient Information. The row for each patient provides demographic information, diagnostic information about their epilepsy, and brain imaging results.

Subject Number	Number of Electrodes Implanted	Number of Electrodes Implanted, by Location			
		Left Hemisphere		Right Hemisphere	
		Frontal	Temporal	Frontal	Temporal
1	16	4	4	4	4
2	16	4	4	4	4
3	16	4	4	4	4
4	12	3	3	3	3
5	14	3	4	3	4
6	11	3	2	3	3
7	2	0	2	0	0
8	4	0	2	0	2
9	12	3	3	3	3

Table 2: Number and placement of implanted electrodes. Each electrode had multiple macro contacts, which are the actual recording surfaces located along the electrode shaft. Therefore, some macro contacts were located closer to the surface of the brain. Note that the macro contacts (6-10 per electrode) were evenly spaced along the electrode shaft.

Subject Number	No. of Electrode Contacts Used in Analysis	No. of Electrode Contacts Used in Analysis, by Location			
		Left Hemisphere		Right Hemisphere	
		Frontal	Temporal	Frontal	Temporal
1	12	3	3	3	3
2	9	2	3	1	3
3	10	2	2	4	2
4	12	4	0	6	2
5	11	4	3	2	2
6	12	3	3	2	4
7	2	0	2	0	0
8	3	0	2	0	1
9	11	3	3	2	3

Table 3: Number and placement of electrode contacts used in analysis. All contacts used were near the outermost ends of their electrodes.

Subject	1	2	3	4	5	6	8	9	7
Minutes of REM Correctly ID'ed	47.5	26.0	14.5	22.5	31.5	62.5	25.0	60.0	NA
Fraction of REM Labels Correct	0.98	0.95	1.00	0.73	0.98	1.00	0.86	0.94	0.00
Fraction of REM Correctly ID'ed	0.77	0.42	0.60	0.40	0.88	0.78	0.79	0.67	NA
Min. Alpha Power Diff. B/W Closest Competing Cluster and REM Cluster	0.79	0.07	0.09	2.00×10^{-3}	0.01	0.07	0.74	0.06	6.00×10^{-3}
Fraction of REM Cluster Electrode Alpha Power Not Minimum	0.00	0.10	0.20	0.08	0.09	0.00	0.00	0.18	0.00
Number of Clusters	14	12	10	14	8	6	14	14	14
Number of Electrode Contacts	12	9	10	12	11	12	3	11	2

Table 4: Information related to REM vs. Wake Sleep Scoring Results. The row labels of the table are as follows.

Minutes of REM Correctly ID'ed: The duration, in minutes, of REM episodes correctly identified by our procedure. **Fraction of REM Labels Correct**: The fraction of REM-labeled episodes that were in fact REM episodes. **Fraction of REM Correctly ID'ed:** The fraction of all REM episodes that were correctly labeled by our procedure. **Min. Alpha Power Diff. B/W Closest Competing Cluster and REM Cluster:** The least alpha power difference among all electrode contacts, where an alpha power difference is calculated for each electrode contact as the alpha power difference between the rank 2 and rank 1 clusters for that electrode contact. A large number indicates a tendency for large alpha power differences to be exhibited for all electrode contacts when comparing the REM cluster with the closest competing cluster. **Fraction of REM Cluster Electrode Alpha Power Not Minimum**: The fraction of electrode contacts for which the

corresponding rank of the REM cluster was not 1. The lower the value, the greater the number of electrode contacts for which the REM cluster was of rank 1. **Number of Clusters**: The number of clusters selected by the clustering procedure. This number minimizes the AIC when selecting among clusterings of size 1 to 14. **Number of Electrode Contacts**: Number of electrodecontacts used for identifying REM episodes for each subject.

FIGURES

A.

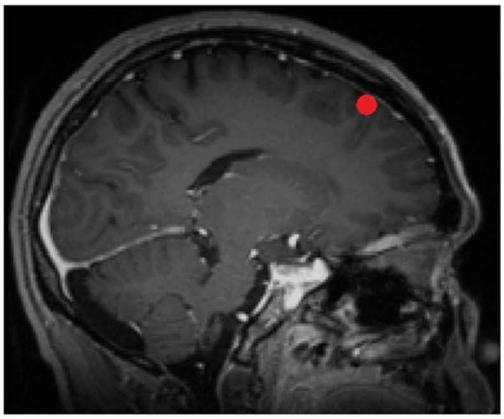

B.

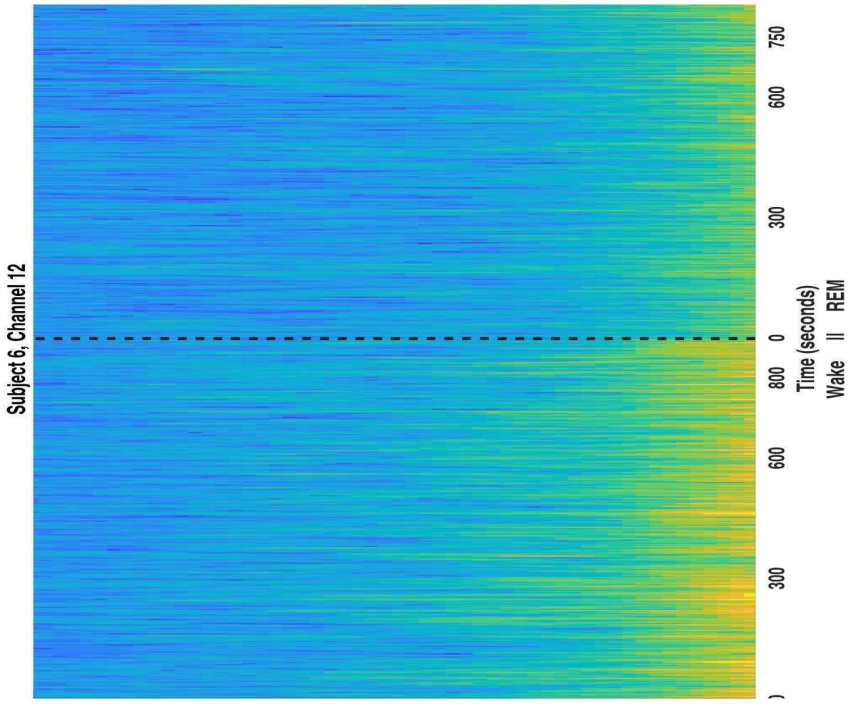
Subject 6, Channel 12
750
600
300
0
800
600
300
Time (seconds)
Wake
REM

Figure 1. Electrode localization and spectrogram. (a) A sagittal MRI image showing the location of the outermost cortical contact of a frontal electrode in the left hemisphere for subject 6; the contact is located in the left superior frontal gyrus. (b) Spectrogram showing the alpha activity pattern detected from this electrode contact during Wake and REM sleep. The black line indicates the beginning of the REM sleep episode. Note that not shown is a large lapse in time—the REM episode occurred much later in the night than the wake period.

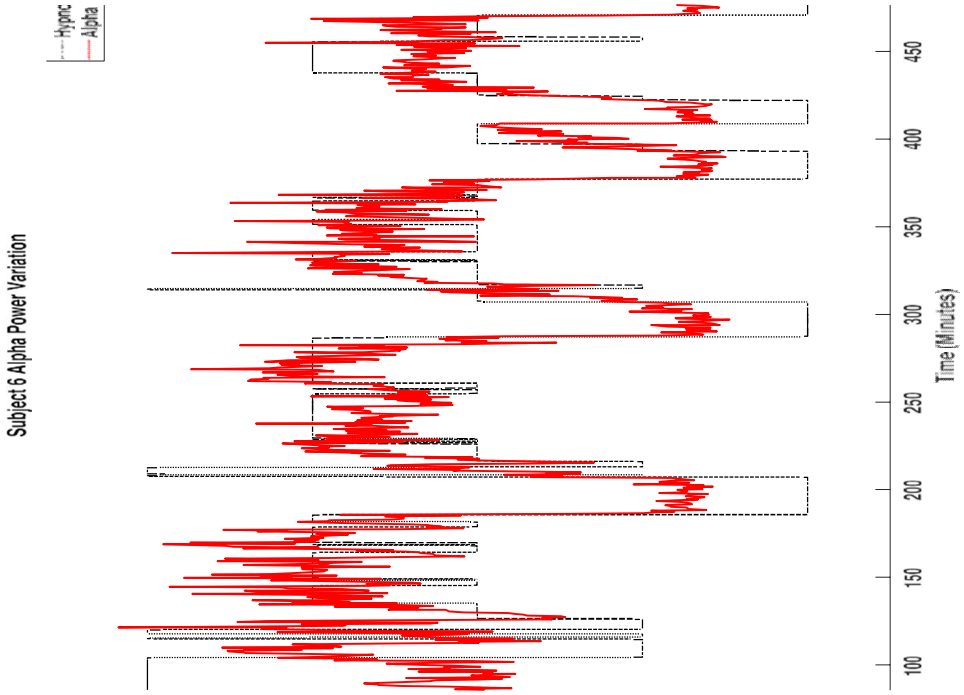

Figure 2. Hypnogram and alpha power variation over time for subject 6. Average Hilbert power variation (red) in the alpha band (8-12Hz) over time, overlayed with manually scored hypnogram (black). Note that during each REM period, alpha power dips below the level seen in Wake.

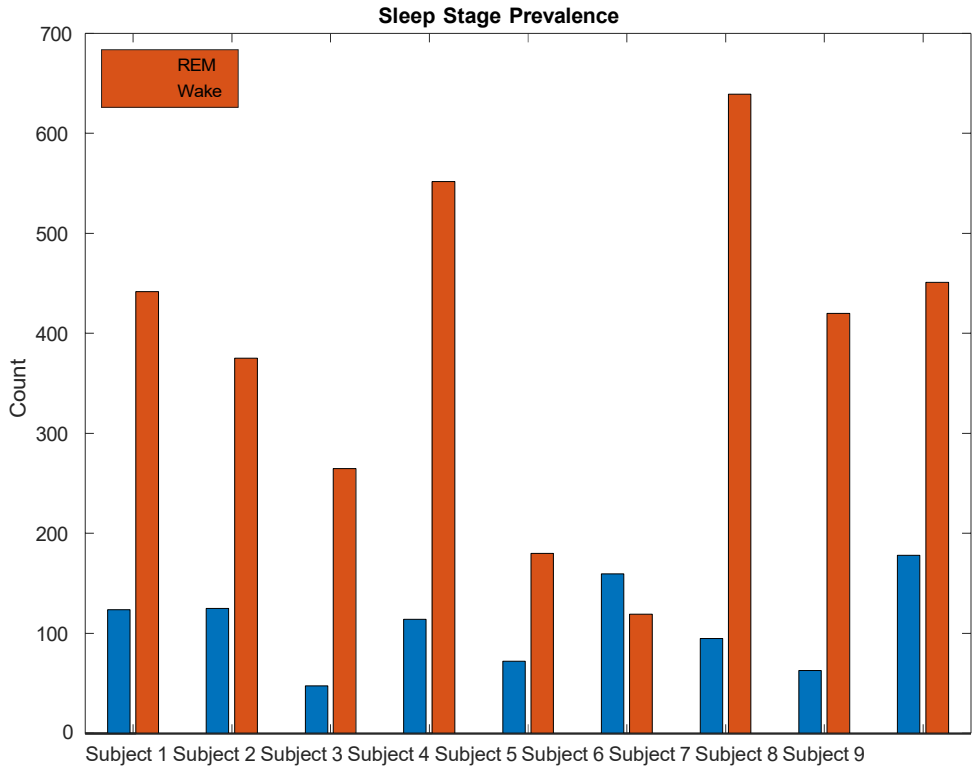

Figure 3. The number of Wake and REM sleep stages for each subject. Except for subject 6, all subjects exhibited more Wake than REM sleep stages. The count is the number of 30-second epochs.

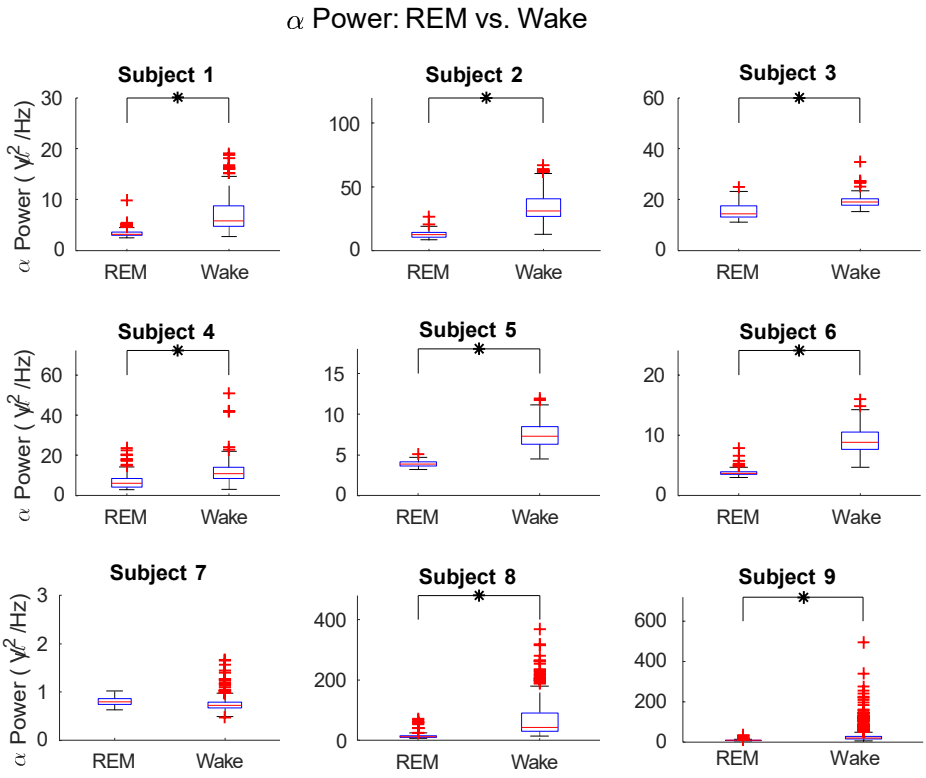

Figure 4. Comparison of alpha (α) power for Wake (W) and REM (R) sleep stages, for each subject. The black asterisk indicates that mean alpha power during Wake was significantly larger than that during REM. All but one subject (i.e., Subject 7) exhibit larger Wake mean alpha power than REM mean alpha power (significant at the 0.05 Bonferroni-corrected significance level; one-sided, unpaired t-test). Subject 7 exhibits abnormal sleep architecture and would be excluded from studies of healthy sleep.

A.

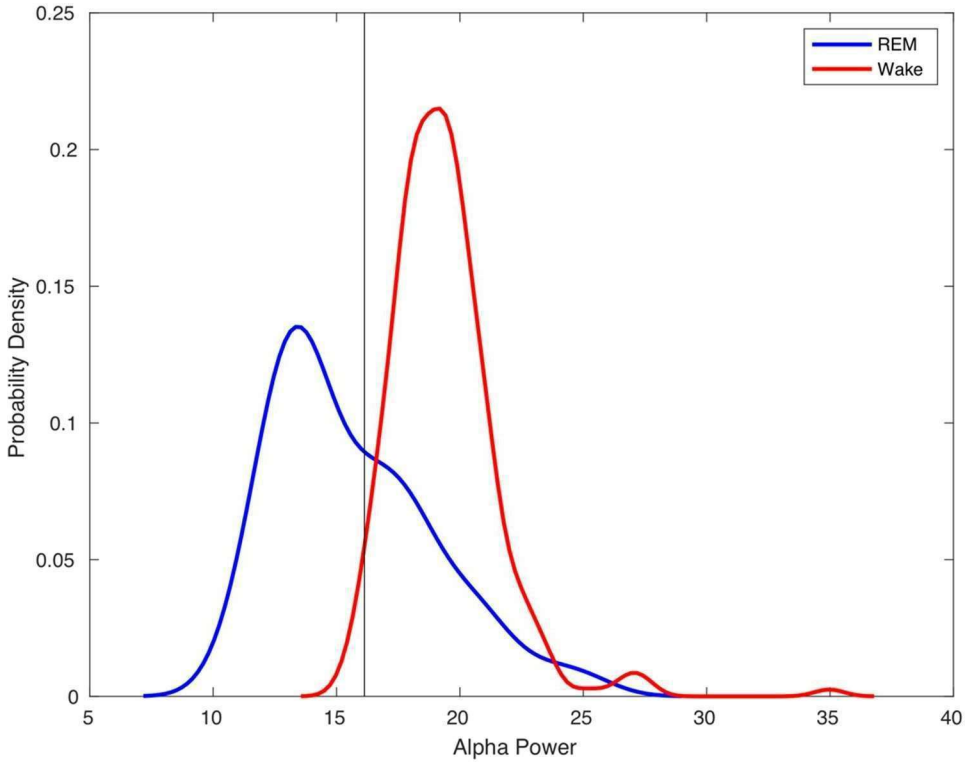
REM
Wake
Probability Density
Alpha Power
0.25
0.2
0.15
0.1
0.05
0
5
10
15
20
25
30
35
40

B.

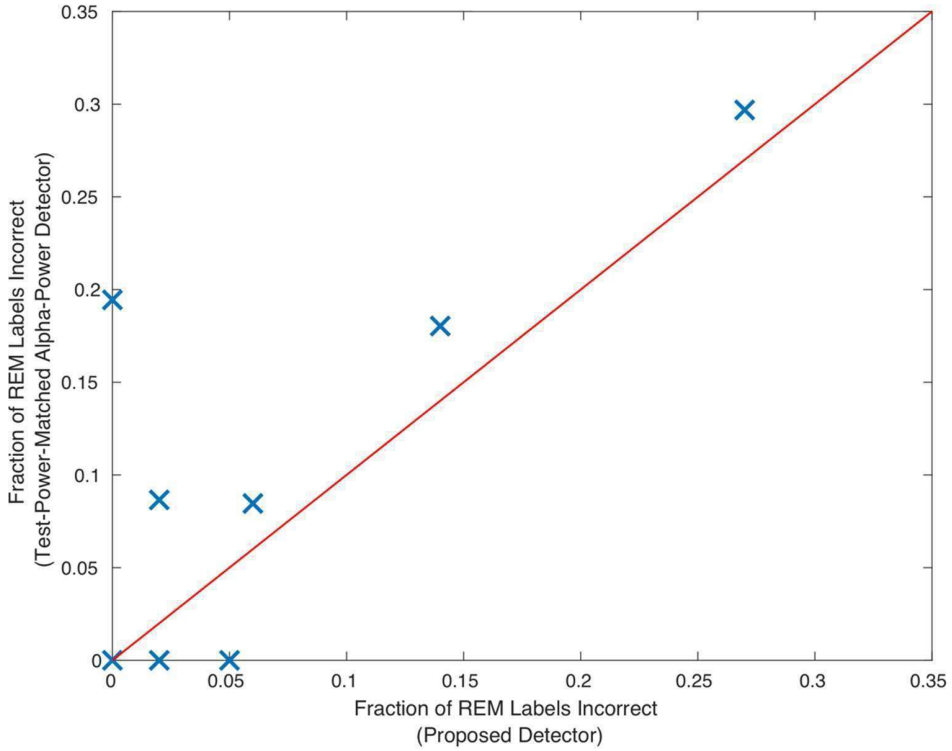
Fraction of REM Labels Incorrect
(Test-Power-Matched Alpha-Power Detector)
Fraction of REM Labels Incorrect
(Proposed Detector)
0.35
0.3
0.25
0.2
0.15
0.1
0.05
0
0
0.05
0.1
0.15
0.2
0.25
0.3
0.35

Figure 5. A. Empirical probability density functions for alpha power from REM epochs (blue trace) and wake epochs (red trace) in subject 3. The black vertical line indicates the alpha power level such that, if episodes with average alpha power below that level are labeled REM, the number of correctly identified REM episodes matches the number identified in the proposed procedure (referred to as Proposed Detector in Figure 5B). B. A direct comparison between the proposed procedure (labeled Proposed Detector) and an alpha-power test (binary hypothesis test) based on average alpha power. The two detectors are matched in statistical power (probability of a correct detection) in the sense that they both correctly label the same number of REM episodes, but they differ in the number of REM labels assigned to Wake episodes. The vertical axis indicates the fraction of all REM labels that are actually assigned to Wake episodes by the alpha-power test, while the horizontal axis indicates the fraction of all REM labels that are actually assigned to Wake episodes by the Proposed Detector. Each mark corresponds to one subject. A mark lying on the red line would indicate equal detector performance for a single subject. For the achieved statistical power, the proposed procedure is superior for five of eight subjects, and only slightly worse for the remaining two (excluding subject 7).

Chapter 3: The Role of Sleep Spindles During Slow-Wave Sleep in Memory Consolidation

Abstract

Sleep spindles are a distinct brainwave pattern observed during stage 2 sleep as well as slow-wave sleep. Historically, sleep spindles were thought to occur synchronously across the brain, in a global manner. In recent research, the use of intracranial EEG has given insight to the idea that sleep spindles may occur at specific times in specific areas in the brain, in a local manner. We employed two standard targeted memory reactivation paradigms to examine the role of local spindles in memory consolidation.

Data were collected from four patients (2 females and 2 males) between the ages of 20 and 56 years (mean 31 years) undergoing invasive monitoring using intracranial depth electrodes for intractable epilepsy. Data (including EOG and EMG recordings) were scored for sleep by experienced sleep scorers and then analyzed for changes in spindling activity following an auditory stimulation during sleep.

Local sleep spindles were identified from our intracranial EEG recordings, confirming that local sleep spindles are observable through intracranial EEG. Following the presentation of an auditory cue during a night of sleep, local sleep spindles were elicited at a specific time. This particular observation was seen for both the declarative and procedural memory tasks.

These results suggest that local sleep spindles may play a role in memory consolidation processes that occur during sleep.

Introduction

An abundance of research on sleep spindles, particularly sleep spindles occurring during SWS, show that both waveforms are strongly tied to the consolidation of memories.[2,7-9,13,14,25-27] Further research has tried to show exactly how sleep spindles promote learning and memory consolidation. One proposed idea is that sleep spindles are involved in the reactivation of clusters of neurons that were activated during learning.[27] This reactivation of neuronal clusters is believed to strengthen hippocampal-cortical connections.[27,28] In doing so, cortical neuron clusters begin to form more integrated memory traces of what was previously learned, thus consolidating them.[25] Likewise, SWS is also thought to play a role in this communication between the cortex and subcortical brain structures like the hippocampus.[29] Despite the amplitude of brain activity during SWS already being the highest among all other stages of sleep, it has been shown to increase when SWS occurs before learning a task.[30-32] Interestingly, slow waves that were artificially generated during NREM sleep using transcranial electrical stimulation to mimic SWS has been shown to improve hippocampally dependent memories.[33]

Another technique to try and artificially manipulate the brain wave patterns occurring during sleep has been developed termed targeted memory reactivation.[11,12,34] What happens in these studies is that a participant performs a memory task while an auditory or odor cue is presented. After the initial memory task, the participant goes to sleep. While they sleep, the researchers replay the stimulus cues presented during the memory task to the sleeping participant while the participant is in SWS. As a result, the researchers found that memory performance on the task improved compared to controls who did not have a stimulus cue presented during sleep.[11,12,34] What has been observed and reported in numerous studies is that the presentation of these cues during sleep can induce the replay of neuronal sequences associated with the cues and there is a direct effect on certain brainwave properties during sleep.[35,36] Specifically, a lot of studies have shown that

targeted memory reactivation produces increased spindle activity and spindle density.[35] Targeted memory reactivation's impact on spindle properties is also believed to play a role in enhancing memory consolidation by biasing the replay of the learned information during sleep.[37,38]

Emerging Evidence of Different Kinds of Sleep Spindles

Past EEG research show that sleep spindles propagate throughout the brain in a synchronous and global manner.[17,18,21-23] However, research using other methods like magnetoencephalography (MEG) and human intracranial recording have shown that sleep spindles may be localized in origin to particular areas of the brain. [18,21,22,24] Additionally, evidence for local slow waves, in addition to local spindles were found by Nir et al. (2011), with local slow waves being more prevalent in later NREM sleep of the night and local spindles being more prevalent in early NREM sleep of the night.[18]

Even though the distinction between local and global spindles has been identified in numerous studies, the functional significance of local spindles remains unanswered.[17] Particularly, the question of whether or not local spindles play a role in memory consolidation is still not well known. There is also a void of knowledge in how local and global spindles relate to each other. Do they interact with each other? Do local spindles serve a different role during sleep than global spindles? We aim to provide more insight into the neural dynamics involved with local and global sleep spindles and their potential role in sleep by using iEEG recording methods and two memory tasks that will test declarative and procedural memory, an object-location memory task and a finger-tapping memory task, respectively. To do so, we will implement two tasks that are known to elicit sleep mediated effects on learning through targeted memory reactivation.[11,12] The utilization of iEEG will not only allow us to observe local spindles, but to investigate deeper brain

structures such as the hippocampus and amygdala that is not afforded to us by typical EEG recordings.[17,18,22]

Materials and Methods

Data for both tasks mentioned previously were collected from four patients (2 females and 2 males) between the ages of 20 and 56 years (mean 31 years) undergoing invasive monitoring using intracranial depth electrodes for intractable epilepsy. Patients signed the informed consent approved by the Institutional Review Board (IRB) at Carilion Roanoke Memorial Hospital prior to participating in the study. Two to sixteen Ad-Tech depth electrodes, each with 6 to 14 macro contacts, were implanted in each subject. Note that the macro contacts are the recording points along the shaft of each electrode and are regularly spaced. Therefore, some macro contacts are located closer to the surface of the brain. The placement of electrodes was determined strictly by clinical criteria without considering research needs. Electrophysiological readings from the Ad-Tech electrodes were received by a 256-channel ATLAS digital acquisition system from Neuralynx (Bozeman, MT), which was connected to a PC running Pegasus Acquisition Software from Neuralynx. The input signals were sampled at 2000 Hz. For each subject, recording started between 8 PM and midnight, depending on an estimated bedtime. EEG data from the raw Neuralynx files were converted to EDF files in blocks of 4-hour periods. For each subject, between 6 to 12 hours of sleep/wake data were recorded and considered for analysis.

Electrode Localization

The locations of depth electrode contacts were determined using Freesurfer[37,38] and IELU software in two steps: reconstruction and coregistration. First, a preoperative high-resolution 7 magnetic resonance imaging (MRI) scan was used to generate a 3D rendering of the subject's brain using FreeSurfer; this rendering was placed in a 3D coordinate system (RAS). During the reconstruction process, FreeSurfer also automatically generates subcortical and cortical parcellations with anatomical labels using the Desikan-Killiany Atlas.[40] Second, the postoperative CT scan was coregistered with the 3D rendering using the IELU pipeline, thus providing a RAS coordinate for

each electrode contact. Using the FreeSurfer-generated parcellations and the RAS coordinates, we determined the anatomical location of each electrode contact with the help of a MATLAB script.[41] A quality check on localization accuracy was performed via visual inspection.

Behavioral Task

For the object-location memory task, which was used by Rudoy et al., the participant will have to learn the object-location pairing of 30 objects.[11] To be more specific, the participant will go through a learning phase where the participant sits in front of a computer screen that shows a checkerboard. On this checkerboard, an object (e.g. an apple) will be located somewhere on the checkerboard. At this time, a sound that characterizes that specific object (e.g., the sound of an apple being eaten), will be played to the participant during this learning phase. This will happen for 30 objects, one after the other, that have characteristic sounds associated with each object. After all 30 object-location pairs are shown to the participant, they are then tasked with remembering where each object was on the checkerboard, and moving the object from the center of the board to the desired location. The participant continues the learning phase of this task until all object-location pairs are learned. Figure 1A shows an example image of the desired location of the apple image, and Figure 1B shows an image of where the apple image starts for the participant to then move to the desired location. During this process, once they correctly identify an object-location pair, it is removed from the list of 30 pairs. This is done to ensure that the information is encoded at some level. After the learning phase, the participant will complete the test phase of the object-location memory task.

In the test phase, the checkerboard will appear on the computer screen, and the 30 object-location pairs will be shown to the participant, one after the other, just like in the learning phase. After all 30 object-location pairs are shown to the participant they must then move the object from the center of the screen to the desired location for all 30 object-location pairs; this is done in the exact same

manner as the learning phase. Once all 30 objects are moved by the participant, the testing phase ends. There is no repetition of showing the participant the desired locations of the object-location pairs, unlike the learning phase.

Object-location pairs will be considered "poorly learned" based on the center-to-center distance the participant placed the object in the testing phase from its exact location, the higher the center-to-center distance, the more poorly learned the object-location pair will be. After the testing phase, the participant will begin the sleeping portion of the study. During the sleeping portion of the study, a sequence of the sounds of the objects mentioned earlier (e.g., the sound of an apple being eaten) will be played to the participant while they are in SWS. The sequence of sounds that play is determined by the participant's performance in the test phase, with the best performing object location pairs starting first, followed by every other sound in order of decreasing performance playing after. This will result in a total of 15 sounds from the list of the 30 object-location pairs being played to the participant. When these 15 sounds are all played to the participant, the same sounds are then replayed to the participant, but this time in a random order for roughly 20-30 minutes of observed SWS. When the participant awakens in the morning, they redo the test phase one last time.

Figure 1A

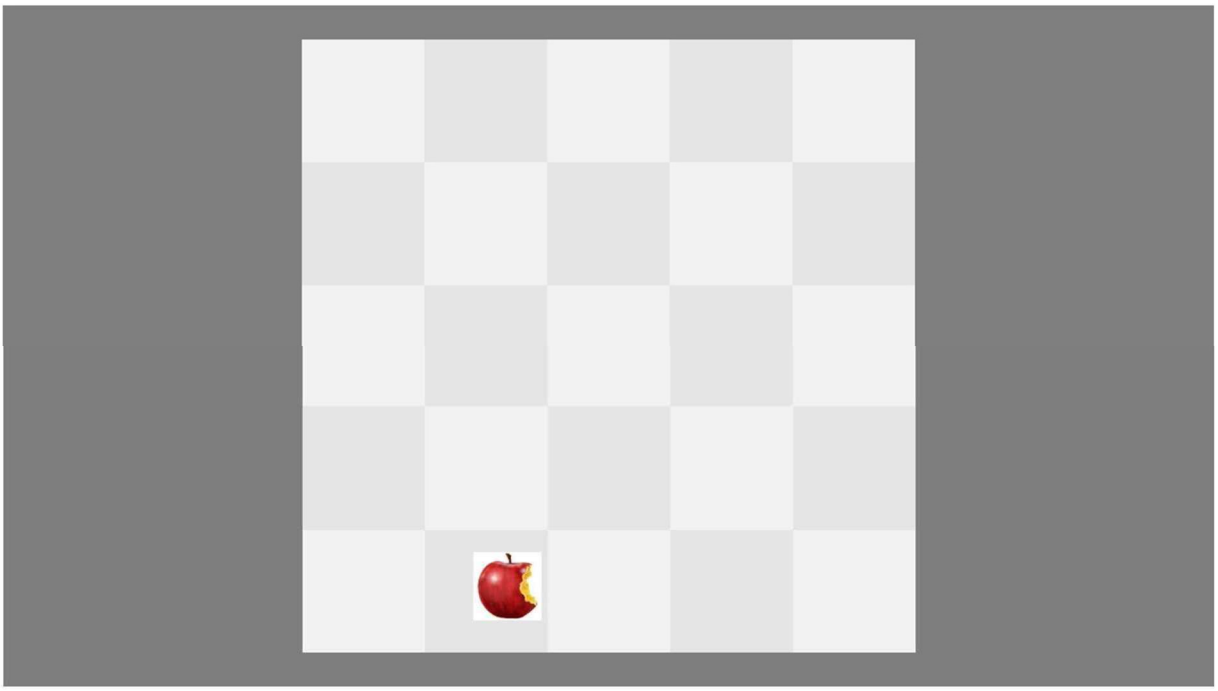

Figure 1B

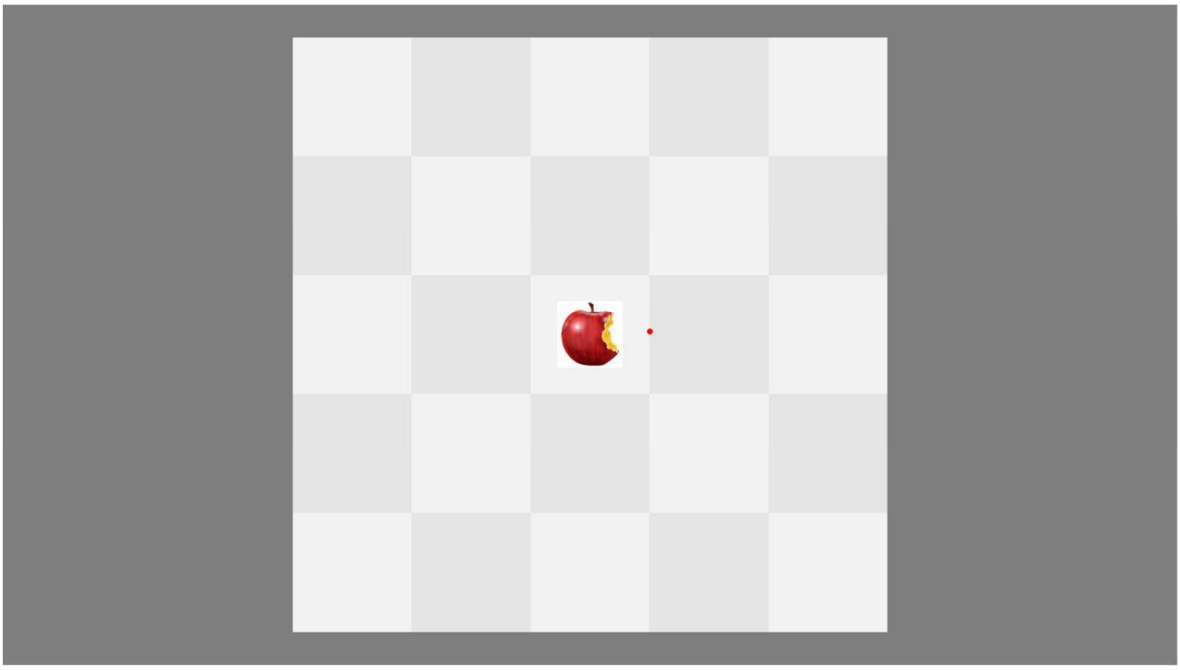

Figure 1. Screenshots from the declarative memory task. Figure 1A shows a section of the learning phase where the participant sees where the image (apple) should be placed. Figure 1B shows a section of the learning phase where the participant must move the image (apple) from the center of the screen to the desired location shown in Figure 1A.

Subjects will also perform a procedural memory task before they go to sleep. They will be retested after they awaken. Note the procedural memory task will be conducted on a different night then the declarative memory task. We will present the task on a small notebook PC that can be used in the hospital room. We will administer a serial reaction time task (SRTT) that is adopted from Cousins et al. (2014).[12] Briefly, subjects will learn two different 12-item finger press sequences, Sequence A (1-2-1-4-2-3-4-1-3-2-4-3) and Sequence B (2-4-3-2-3-1-4-2-3-1-4-1); additionally, a random sequence of tones will be presented to the participant. The numbers correspond to specific fingers on the left hand. Subjects are presented one of four different pictures in one of four locations. Figure 2 shows an example of what the participant sees on the computer screen. The same pictures will be used for both sequences, and a given picture always occurs in the same location. Each picture is accompanied by a unique sound, with the sounds for one sequence consisting of high-pitched tones and the sounds for the other consisting of low-pitched tones. Subjects will be asked to press the appropriate keys, indicated by the locations of the pictures, as quickly as possible, while keeping their errors to a minimum. Following the task, we will record the subject's sleep and either the sequence of sounds for Sequence A or the sequence of sounds for Sequence B during NREM sleep will be randomly chosen to play during their sleep. When the subjects awaken, we will retest them on the SSRT task. The parameters for sound presentation

during sleep and the counterbalancing and control measures adopted from Cousins et al. will be used (2014).[12]

The participant will go to sleep in the hospital while still being recorded with iEEG, EOG, and EMG electrodes. When the participant falls asleep, their brain waves will be monitored by the researcher. By combining these three recording techniques, a trained sleep researcher can tell the difference between the brain wave activity of different sleep stages. For the purposes of this study, the brain wave activity of the participant will let the experimenter know when the participant has entered (SWS). When the participant enters SWS, the sound cues will be played, as described previously.

Figure 2

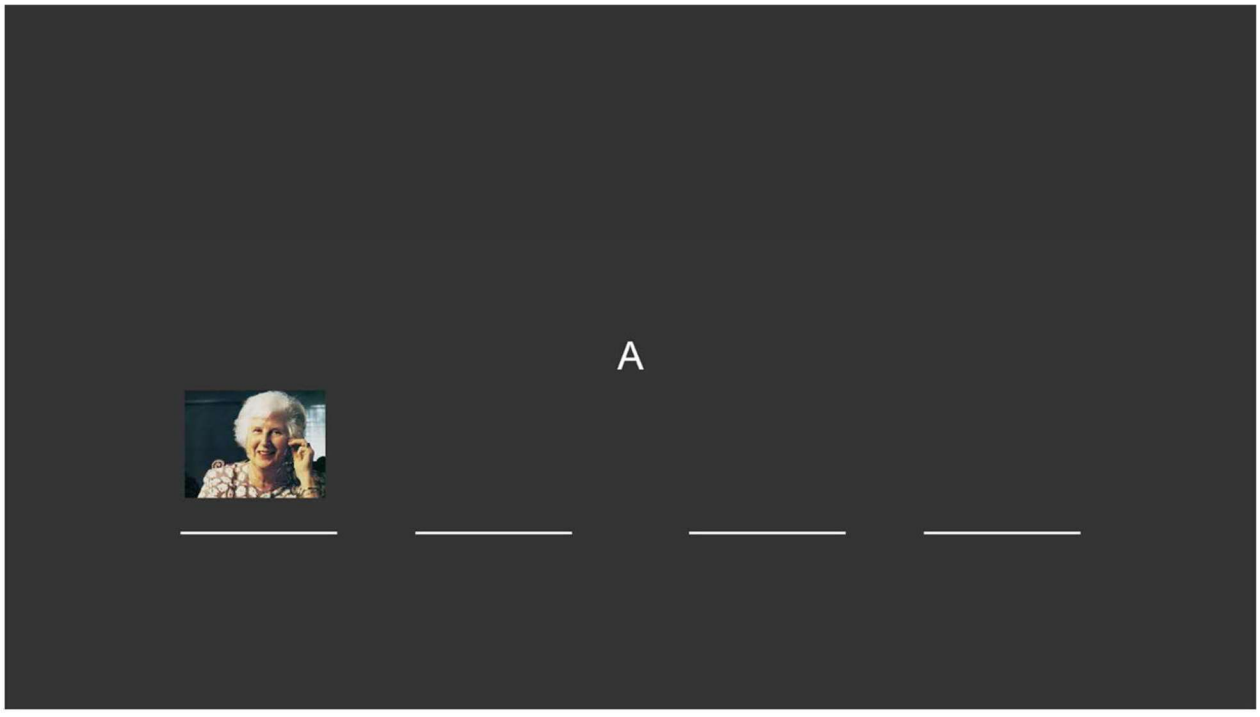

Figure 2. An example image of what the participant sees in the procedural memory task. In this example, the participant would press the left most button on the button box, corresponding to input 1 in Sequence A.

Data Analysis

Defining Local Spindles

Before we can investigate the neural dynamics of local vs global spindles, we first need to define what exactly a local sleep spindle is. We use a definition similar to the one used by Nir et al. A local sleep spindle is defined as a sleep spindle that occurs in less than 50% of electrode recording sites at a particular time.[17,18] The process of selecting contacts for detecting local and global spindles is described below for one subject, for illustrative purposes. In subject 4, we initially had 127 clinically available electrodes, seven of which were not iEEG channels (EMG, EOGs, EKGs, etc.) and were not used for analyzing spindling activity. The remaining 120 channels were arranged in a bipolar montage that was then run through our channel selection process. Only electrodes applied to gray matter areas of the brain were selected which decreased the number of electrodes to 48. Next, to determine which of these channels have spindling activity over the course of the experiment, an automated system generated power spectrums for each electrode for every two seconds of data. Figure 3A and 3B show examples of power spectrums for bipolar electrodes that elicit spindling activity and bipolar electrodes that do not elicit spindling activity, respectively. These power spectrums were averaged over to form one power spectrum for each electrode which were then fitted to a 1/f model, as done in previous papers.[17] Electrodes that had deviations from this 1/f model in the spindle frequency band were then chosen as electrodes with spindling activity; this dropped the number of electrodes from 48 to 41.

Figure 3A

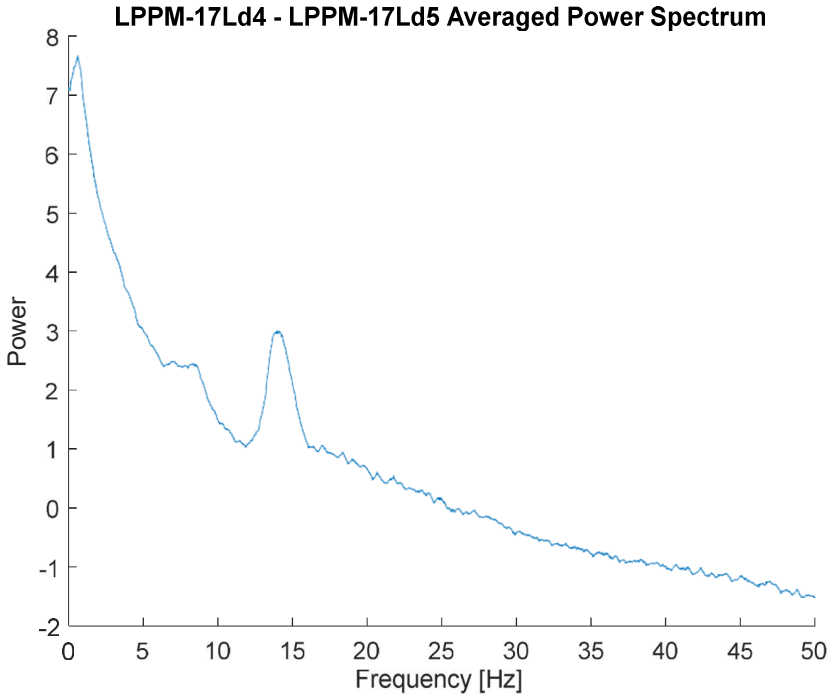
LPPM-17Ld4 - LPPM-17Ld5 Averaged Power Spectrum
Power
Frequency [Hz]
8
7
6
5
4
3
2
1
0
-1
-2
0
5
10
15
20
25
30
35
40
45
50

Figure 3B

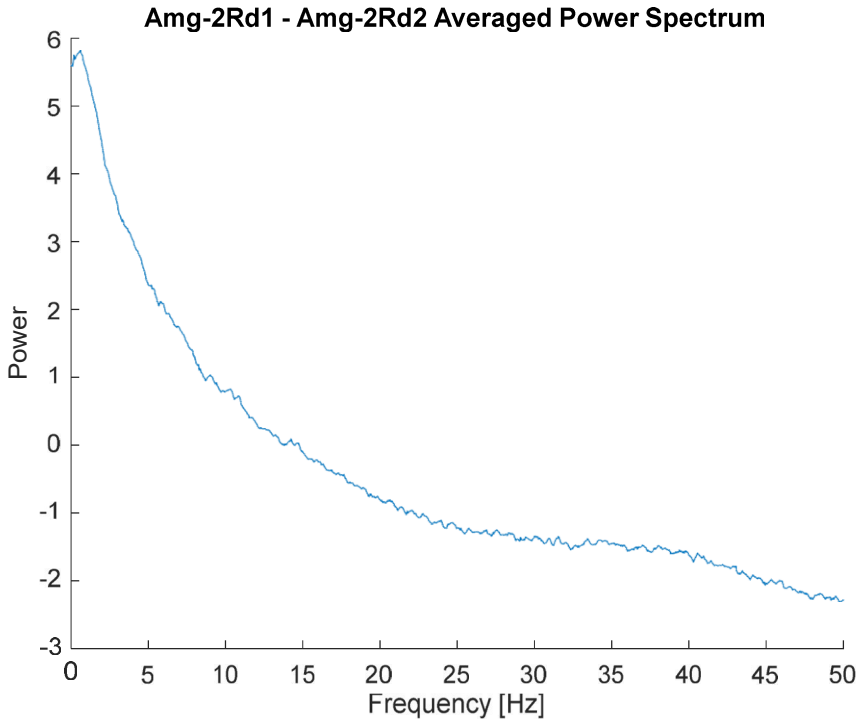

Figure 3. Averaged power spectrums of two different bipolar electrodes during a duration of N2 sleep from iEEG recordings. Figure 3A shows the power spectrum of an electrode that elicits a sleep spindle throughout the section of data. Figure 3B shows the power spectrum of an electrode that did not elicit sleep spindle activity through the section of data (note the band occurring around the frequency range of sleep spindles, 11-16Hz).

To identify global vs. local spindles, these 41 channels were then run through a custom algorithm for detecting spindles in time. This algorithm goes through each electrode in time over the course of the experiment and identifies if there is a sleep spindle at a specific point. For each electrode, if a spindle is detected at same time point, that spindle gets added to the pool of electrodes that detected a sleep spindle at that time. After every electrode is taken into account, the final number

of electrodes that elicited a spindle at that time is divided by 41, the total number of channels that elicit spindling activity. A global spindle is detected at a specific time point in the recording if this number divided by 41 is greater than or equal to 0.5 (50%). Figure 2 shows the result of this custom algorithm and shows an example of local and global sleep spindling.

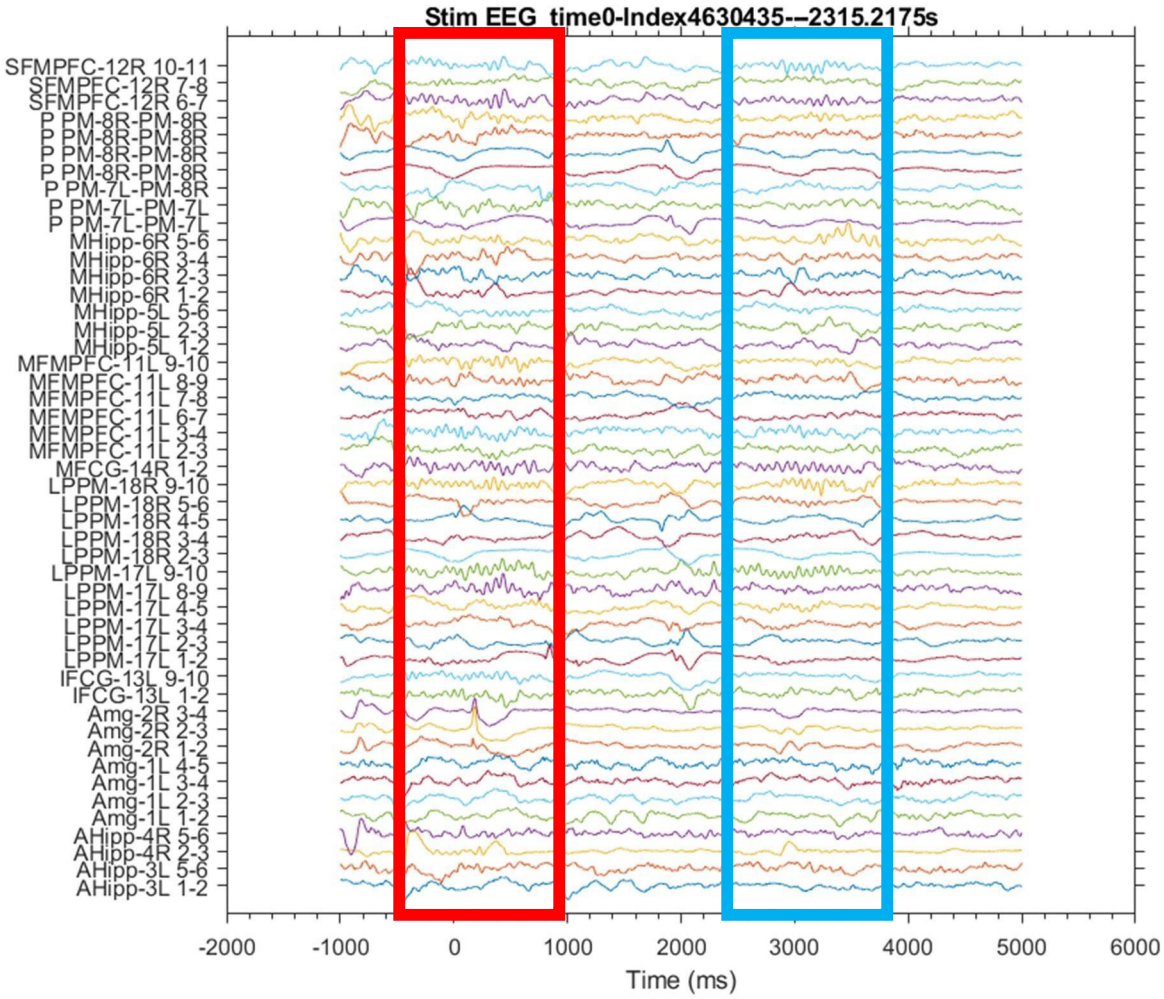

Figure 4. Image generated in MATLAB showing a segment of a sleep recording of global vs. local sleep spindles. The section outlined in the red rectangle is a section of sleep where sleep spindles occurred in more than 50% of iEEG channels (global spindling). The section outlined in blue shows a section of sleep where sleep spindles occurred in less than 50% of iEEG channels (local

spindling).Based on figures 3 and 4, we demonstrate that local spindles are identifiable through the use of iEEG recordings.

Results

As seen by others, we found that the majority of detections are local sleep spindles. We utilized the spindle detection algorithm described in the methods section for detecting spindles in specific channels in time during a recording. For each detected spindle, the fractional coverage is determined and binned into a histogram. Figure 5 shows the results of this process for one subject for one night of sleep. As can be seen by this figure, high spindle counts fall below 50% of fractional coverage (i.e., spindles detected in less than half of the 41 channels described previously). Also of note is that most spindle counts are rarely seen at or above 80% fractional coverage.

Figure 5

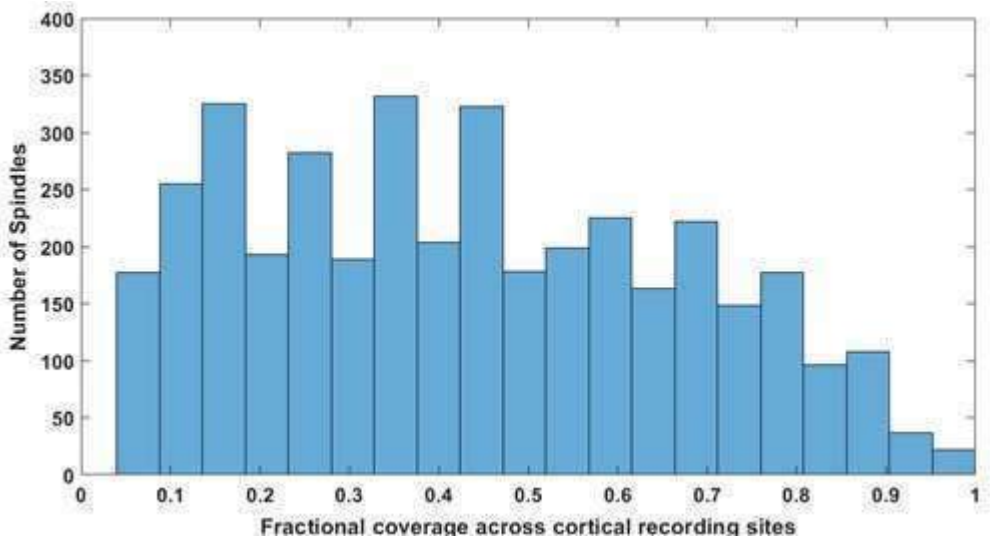

Figure 5. Histogram showing detected spindle counts from our custom algorithm. This histogram shows that most spindle counts fall below the local spindle threshold of less than 50% fractional coverage. Spindle detection 80% or higher fractional coverage is rarely seen.

Now that we have shown local spindles can be identified through iEEG recordings and that local spindles are more prevalent than global spindles, the next step is to see how they are affected by the auditory stimulations of our experiments. Figure 6A shows a spectrogram of data acquired before and after the presentation of an auditory stimulation (time 0) for the declarative memory task. This data was averaged over 53 different auditory stimulation events during a night of recording. From this spectrogram we can see that there is an increase in spindle power following the auditory stimulation (warmer colors around time 1000ms). Figure 6B shows another histogram of the spindles detected in figure 6A and indicates the fractional coverage of these spindles. This histogram shows that the distribution of sleep spindles is more local than global. Likewise, for the procedural memory task, we roughly see the same thing as in the declarative memory task. Figure 7A shows a spectrogram of data acquired before and after an auditory stimulus occurred during sleep. The data in the spectrogram occurred only during the first tone of the 12-tone sequence (time 0), over 12 different sequences; this data is then averaged together. We can see in this spectrogram as well that there is an increase in spindle power following the auditory stimulation around 1000ms. Figure 7B shows the spindle detection distribution for the data and, again, illustrates that most of the spindles occurring during this time are local spindles.

Figure 6A

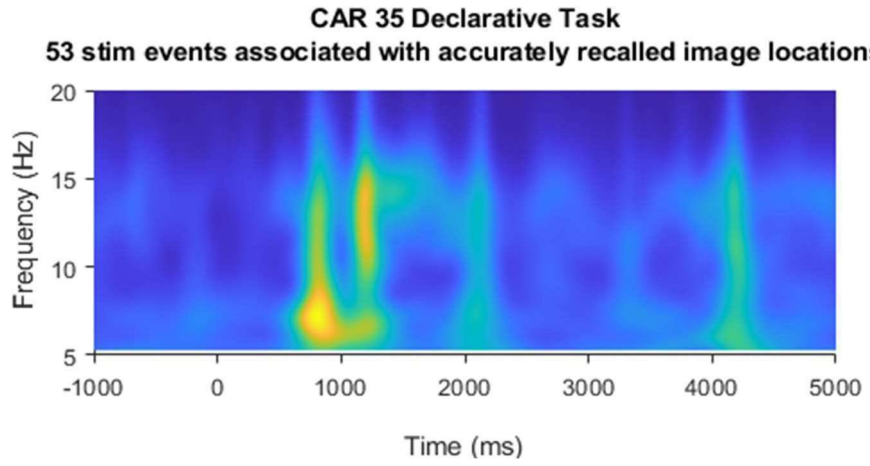

Figure 6B

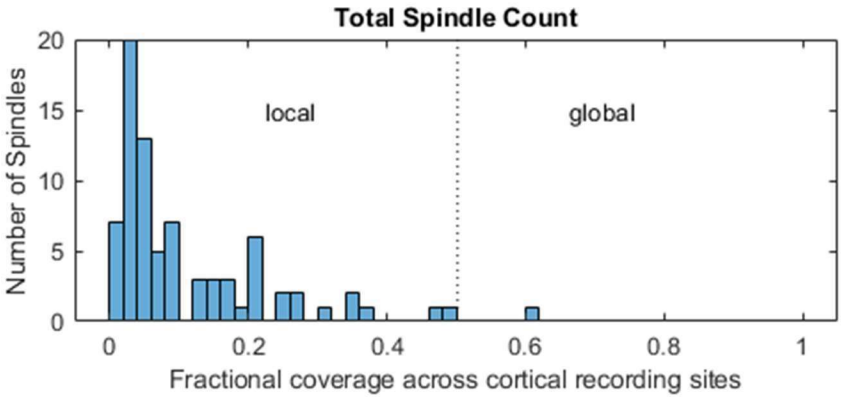

Figure 6. Figure 6A shows the spectrogram of six seconds of data. The first second of data is before the presentation of an auditory stimulus (time 0). This time period of data was taken from 53 different auditory stimulations of object-location pairs that were accurately recalled in the testing phase of the declarative memory task prior to going to sleep. After the presentation of the stimulus, warmer colors emerge in the spindle frequency band (11 – 16Hz) roughly one second after the presentation of the auditory stimulus. Figure 6B is a histogram that shows that the spindling occurring after the stimulus event is made up of local sleep spindles and not global sleep spindles.

Figure 7A

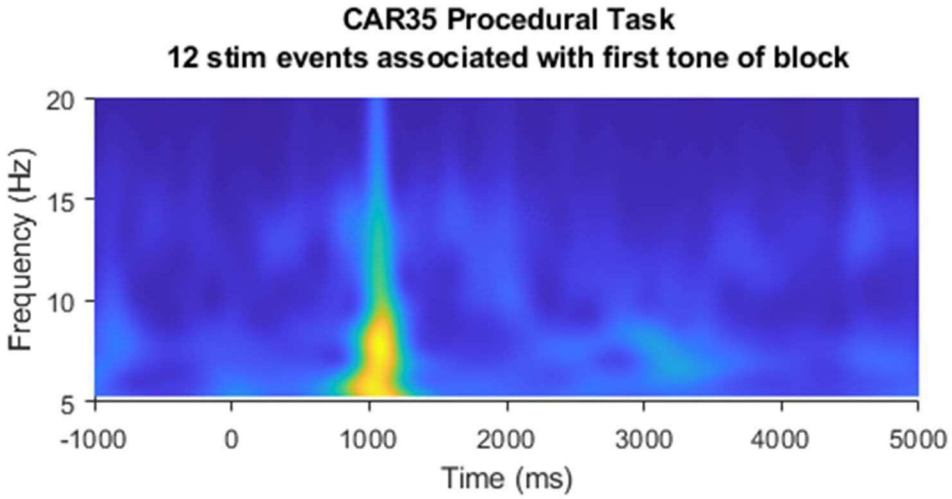

Figure 7B

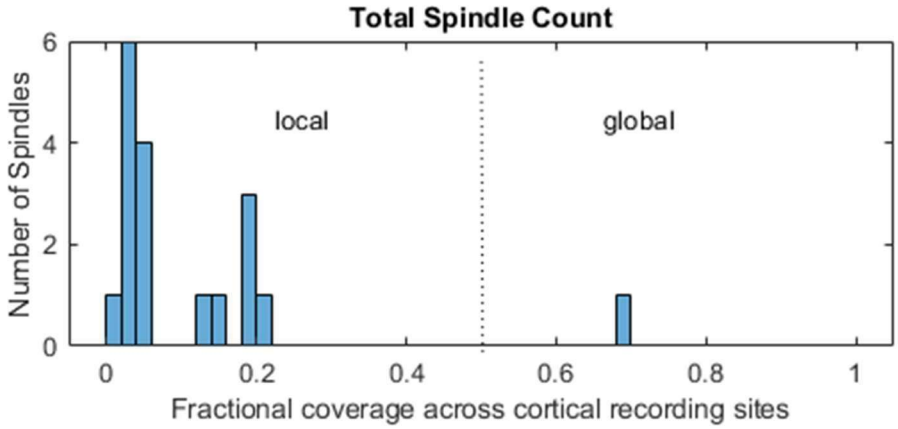

Figure 7. Figure 7A shows the spectrogram of six seconds of data. The first second of data is before the presentation of an auditory stimulus (time 0). This time period of data was taken from the first tone of a 12-tone sequence, 12 times and averaged together. After the presentation of the stimulus, warmer colors emerge in the spindle frequency band (11 – 16Hz) roughly one second after the presentation of the auditory stimulus. Figure 7B is a histogram that shows that the spindling occurring after the stimulus event is made up of local sleep spindles and not global sleep spindles.

Discussion

The purpose of this research was to investigate the neural changes involved with local versus global sleep spindles. We have shown that local sleep spindles are identifiable through the use of iEEG. We have also provided additional evidence that local sleep spindles are more dominant over the course of a night compared to global sleep spindles and our preliminary results show that auditory stimuli induces local spindles at specific times.

Existing limitations of this research, however, include the sample size of this research being low, with only four patients having analysis completed on their sleep recordings. This project also does not go into too much depth about how local spindles are involved in memory and learning. These preliminary findings do show that local spindles occur following auditory stimulation in a targeted memory reactivation related study for both procedural and declarative memory. However, no conclusions can be made on the functional significance during targeted memory reactivation from this study, but it paves the way for future studies to investigate the effect that local spindles have on learning and memory.

Chapter 4: Conclusion

The goal of this research project was twofold. First, we aimed to see if alpha waves observed through iEEG recordings are different across different states of arousal and to examine whether this difference in alpha power can be leveraged for sleep staging. After collecting iEEG recordings from epileptic patients, alpha waveforms were characterized and then used to identify episodesof wake as separate from episodes of REM sleep. Prior to our work, this could only be done if EOG and EMG electrodes were applied to the patient, but in typical iEEG recording setups, EOGs and EMGs are rarely utilized.

On average, we found that alpha power is greater during wake periods than during REM sleep in specific regions. After identifying this difference in alpha power during wake versus during REM sleep, we used this difference to establish a novel clustering method that was able to reliably identify periods of REM sleep in human subjects using iEEG recordings.

Through the development of this method to use the observed differences in alpha wave power between wake and REM sleep states as a way to distinguish between wake and REM sleep states, we made it possible to sleep score iEEG recordings that do not use EOG and EMG electrodes. This not only opens the door for future iEEG recordings to be used for sleep studies, but also allows a wide database of already existing iEEG recordings to be used for sleep research purposes.

Our second goal of this research project was to use iEEG recordings as a reliable way to identify local vs. global sleep spindles in humans. Additionally, we wanted to glean insight into the role that local sleep spindles may play in learning and memory using two standard targeted memory reactivation tasks; one task to test declarative memory and another task to test procedural memory. In standard EEG recordings, local sleep spindles are not able to be identified. From our research, we showed that local sleep spindles are identifiable through the use of iEEG recordings. In addition

to local spindles being identified through iEEG, we showed that local sleep spindles actually occur more often than global sleep spindles.

Preliminarily, we found that the presentation of an auditory cue during SWS, a standard method in targeted memory reactivation studies, has an effect on local sleep spindles. By using spectrogram analysis, we found higher power values of waveforms in the sleep spindle frequency band (11 – 16 Hz) at specific time windows after stimulation. We also found that the sleep spindles occurring from the auditory cue are local sleep spindles, not global. This confirms previous research that local sleep spindles may play a role in the neural processes of learning and memory that occur during sleep.

Due to our low sample size, the investigation of the role that local sleep spindles play in learning and memory was limited. Future research should aim to investigate to what extent local sleep spindles play a part in learning and memory. In addition, future research should also investigate the potential interactions that local sleep spindles have with global sleep spindles. Future research of the lab will investigate the effects of targeted memory reactivation on hippocampal ripples, a distinct waveform found in sleep that is thought to play a role in learning and memory and may have some interaction with sleep spindles.[32,62,72,76]

Bibliography

1. Cirelli, C., & Tononi, G. (2008). Is sleep essential? *PLoS Biology*, *6*(8). https://doi.org/10.1371/journal.pbio.0060216
2. Rasch, B., & Born, J. (2013). About sleep's role in memory. *Physiological Reviews*, *93*(2), 681–766. https://doi.org/10.1152/physrev.00032.2012
3. Nayak CS, Anilkumar AC. EEG Normal Sleep. [Updated 2022 May 29]. In: StatPearls [Internet]. Treasure Island (FL): StatPearls Publishing; 2022 Jan-. Available from: https://www.ncbi.nlm.nih.gov/books/NBK537023/
4. Bailey, D. R., & Attanasio, R. (2012). The history of sleep medicine. *Dental Clinics of North America*, *56*(2), 313–317. https://doi.org/10.1016/j.cden.2012.02.004
5. Loomis, A. L., Harvey, E. N., & Hobart, G. A. (1937). Cerebral states during sleep, as studied by human brain potentials. *Journal of Experimental Psychology*, *21*(2), 127–144. https://doi.org/10.1037/h0057431
6. Dement, W., & Kleitman, N. (1957). Cyclic variations in EEG during sleep and their relation to eye movements, body motility, and dreaming. *Electroencephalography and Clinical Neurophysiology*, *9*(4), 673–690. https://doi.org/10.1016/0013-4694(57)90088-3
7. Girardeau G, Lopes-Dos-Santos V. Brain neural patterns and the memory function of sleep. Science. 2021 Oct 29;374(6567):560-564. doi: 10.1126/science.abi8370. Epub 2021 Oct 28. PMID: 34709916; PMCID: PMC7611961.
8. Berres S, Erdfelder E. The sleep benefit in episodic memory: An integrative review and a meta-analysis. Psychol Bull. 2021 Dec;147(12):1309-1353. doi: 10.1037/bul0000350. PMID: 35404637.

9. Cousins JN, Fernández G. The impact of sleep deprivation on declarative memory. Prog Brain Res. 2019;246:27-53. doi: 10.1016/bs.pbr.2019.01.007. Epub 2019 Mar 21. PMID: 31072562.

10. Jiang F (2019) Sleep and early brain development. Annals of Nutrition and Metabolism 75:44–54.

11. Rudoy JD, Voss JL, Westerberg CE, Paller KA (2009) Strengthening individual memories by reactivating them during sleep. Science 326:1079–1079.

12. Cousins JN, El-Deredy W, Parkes LM, Hennies N, Lewis PA (2014) Cued memory reactivation during slow-wave sleep promotes explicit knowledge of a motor sequence. Journal of Neuroscience 34:15870–15876.

13. Klinzing JG, Niethard N, Born J. Mechanisms of systems memory consolidation during sleep. Nat Neurosci. 2019 Oct;22(10):1598-1610. doi: 10.1038/s41593-019-0467-3. Epub 2019 Aug 26. Erratum in: Nat Neurosci. 2019 Sep 11;: PMID: 31451802.

14. Zhang Y, Gruber R. Can Slow-Wave Sleep Enhancement Improve Memory? A Review of Current Approaches and Cognitive Outcomes. Yale J Biol Med. 2019 Mar 25;92(1):63-80. PMID: 30923474; PMCID: PMC6430170.

15. Latreille, V., von Ellenrieder, N., Peter-Derex, L., Dubeau, F., Gotman, J., & Frauscher, B. (2020). The human K-complex: Insights from combined scalp-intracranial EEG Recordings. *NeuroImage*, *213*, 116748.

16. Ruby P, Eskinazi M, Bouet R, Rheims S, Peter-Derex L. Dynamics of hippocampus and orbitofrontal cortex activity during arousing reactions from sleep: An intracranial electroencephalographic study. Hum Brain Mapp. 2021 Nov;42(16):5188-5203. doi: 10.1002/hbm.25609. Epub 2021 Aug 6. PMID: 34355461; PMCID: PMC8519849.

17. Andrillon T, Nir Y, Staba RJ, Ferrarelli F, Cirelli C, Tononi G, Fried I (2011) Sleep spindles in humans: Insights from intracranial EEG and unit recordings. Journal of Neuroscience 31:17821–17834.

18. Nir Y, Staba RJ, Andrillon T, Vyazovskiy VV, Cirelli C, Fried I, Tononi G (2011) Regional slow waves and spindles in human sleep. Neuron 70:153–169.

19. von Ellenrieder, N., Peter-Derex, L., Gotman, J., & Frauscher, B. (2022). Sleepseeg: Automatic sleep scoring using intracranial EEG recordings only. *Journal of Neural Engineering*, *19*(2), 026057. https://doi.org/10.1088/1741-2552/ac6829

20. Iber C, Ancoli-Israel S, Chesson AL, Jr., Quan SF for the American Academy of Sleep Medicine. The AASM manual for the scoring of sleep and associated events: rules, terminology and technical specifications. 1st ed. Westchester, IL: American Academy of Sleep Medicine; 2007

21. Dehghani N, Cash SS, Rossetti AO, Chen CC, Halgren E (2010) Magnetoencephalography demonstrates multiple asynchronous generators during human sleep spindles. Journal of Neurophysiology 104:179–188.

22. Fernandez LM, Lüthi A (2020) Sleep spindles: Mechanisms and functions. Physiological Reviews 100:805–868.

23. Dehghani N, Cash SS, Halgren E (2011) Emergence of synchronous EEG spindles from asynchronous MEG spindles. Human Brain Mapping 32:2217–2227.

24. Fernandez LMJ, Lüthi A. Sleep Spindles: Mechanisms and Functions. Physiol Rev. 2020 Apr 1;100(2):805-868. doi: 10.1152/physrev.00042.2018. Epub 2019 Dec 5. PMID: 31804897.

25. Diekelmann, S., & Born, J. (2010). *The memory function of sleep. Nature Reviews Neuroscience, 11(2), 114–126.* doi:10.1038/nrn2762

26. Antony, J. W., Schönauer, M., Staresina, B. P., & Cairney, S. A. (2018). Sleep Spindles and Memory Reprocessing. Trends in Neurosciences. doi: 10.1016/j.tins.2018.09.012

27. Wei Y, Krishnan GP, Komarov M, Bazhenov M. Differential roles of sleep spindles and sleep slow oscillations in memory consolidation. PLoS Comput Biol. 2018 Jul 9;14(7):e1006322. doi: 10.1371/journal.pcbi.1006322. PMID: 29985966; PMCID: PMC6053241.

28. Cowan E, Liu A, Henin S, Kothare S, Devinsky O, Davachi L. Sleep Spindles Promote the Restructuring of Memory Representations in Ventromedial Prefrontal Cortex through Enhanced Hippocampal-Cortical Functional Connectivity. J Neurosci. 2020 Feb 26;40(9):1909-1919. doi: 10.1523/JNEUROSCI.1946-19.2020. Epub 2020 Jan 20. PMID: 31959699; PMCID: PMC7046449.

29. Diekelmann, S., & Born, J. (2010). The memory function of sleep. Nature Reviews Neuroscience, 11(2), 114–126. doi:10.1038/nrn2762

30. Huber, R., Felice Ghilardi, M., Massimini, M. *et al.* Local sleep and learning. *Nature* **430**, 78–81 (2004). https://doi.org/10.1038/nature02663

31. Mölle M, Marshall L, Gais S, Born J. Learning increases human electroencephalographic coherence during subsequent slow sleep oscillations. Proc Natl Acad Sci U S A. 2004 Sep 21;101(38):13963-8. doi: 10.1073/pnas.0402820101. Epub 2004 Sep 8. PMID: 15356341; PMCID: PMC518860.

32. Mölle M, Eschenko O, Gais S, Sara SJ, Born J. The influence of learning on sleep slow oscillations and associated spindles and ripples in humans and rats. Eur J Neurosci. 2009

Mar;29(5):1071-81. doi: 10.1111/j.1460-9568.2009.06654.x. Epub 2009 Feb 24. PMID: 19245368.

33. Marshall, L., Helgadóttir, H., Mölle, M. *et al.* Boosting slow oscillations during sleep potentiates memory. *Nature* **444**, 610–613 (2006). https://doi.org/10.1038/nature05278

34. Hu X, Cheng LY, Chiu MH, Paller KA. Promoting memory consolidation during sleep: A meta-analysis of targeted memory reactivation. Psychol Bull. 2020 Mar;146(3):218-244. doi: 10.1037/bul0000223. PMID: 32027149; PMCID: PMC7144680.

35. Malkani, R. G., & Zee, P. C. (2020). Brain Stimulation for Improving Sleep and Memory. Sleep Medicine Clinics. doi:10.1016/j.jsmc.2019.11.002

36. Dale AM, Fischl B, Sereno MI (1999) Cortical surface-based analysis. NeuroImage 9:179–194.

37. Fischl B, Salat DH, Busa E, Albert M, Dieterich M, Haselgrove C, van der Kouwe A, Killiany R, Kennedy D, Klaveness S, Montillo A, Makris N, Rosen B, Dale AM (2002) Whole brain segmentation. Neuron 33:341–355.

38. LaPlante RA, Tang W, Peled N, Vallejo DI, Borzello M, Dougherty DD, Eskandar EN, Widge AS, Cash SS, Stufflebeam SM (2016) The interactive electrode localizationutility: Software for automatic sorting and labeling of intracranial subdural electrodes. International Journal of Computer Assisted Radiology and Surgery 12:1829–1837.

39. Desikan RS, Ségonne F, Fischl B, Quinn BT, Dickerson BC, Blacker D, Buckner RL, Dale AM, Maguire RP, Hyman BT, Albert MS, Killiany RJ (2006) An automated labeling system for subdividing the human cerebral cortex on MRI scans into gyral based regions of interest. NeuroImage 31:968–980.

40. Jain S. Investigation of Sleep Neural Dynamics in Intracranial EEG Patients. Blacksburg, VA: Virginia Tech; 2021.

41. *Chronux*. Chronux Home. (n.d.). Retrieved October 2, 2022, from http://chronux.org/ 42.Mitra, P., & Bokil, H. (2008). *Observed brain dynamics*. Oxford University Press.

43.1. Berger H. On the electroencephalogram of man. *Electroen Clin Neuro*. Published online 1969:Suppl 28:37+.

44. Wright KP, Badia P, Wauquier A. Topographical and Temporal Patterns of Brain Activity During the Transition From Wakefulness to Sleep. *Sleep*. 1995;18(10):880-889. doi:10.1093/sleep/18.10.880

45. Putilov AA, Donskaya OG. Alpha attenuation soon after closing the eyes as an objective indicator of sleepiness. *Clin Exp Pharmacol P*. 2014;41(12):956-964. doi:10.1111/1440-1681.12311

46. Gennaro LD, Ferrara M, Bertini M. The boundary between wakefulness and sleep: quantitative electroencephalographic changes during the sleep onset period. *Neuroscience*. 2001;107(1):1-11. doi:10.1016/s0306-4522(01)00309-8

47. Iber C, Ancoli-Israel S, Chesson AL, Quan SF. The New Sleep Scoring Manual–The Evidence Behind The Rules. *J Clin Sleep Med*. 2007;03(02):107-107. doi:10.5664/jcsm.26812

48. Silber MH, Ancoli-Israel S, Bonnet MH, et al. The Visual Scoring of Sleep in Adults. *J Clin Sleep Med*. 2007;03(02):121-131. doi:10.5664/jcsm.26814

49. Peever J, Fuller PM. The Biology of REM Sleep. *Curr Biol*. 2017;27(22):R1237-R1248. doi:10.1016/j.cub.2017.10.026

50. Nir Y, Tononi G. Dreaming and the brain: from phenomenology to neurophysiology. *Trends Cogn Sci*. 2010;14(2):88-100. doi:10.1016/j.tics.2009.12.001

51. Blumberg MS, Lesku JA, Libourel PA, Schmidt MH, Rattenborg NC. What Is REM Sleep? *Curr Biol*. 2020;30(1):R38-R49. doi:10.1016/j.cub.2019.11.045

52. Siegel JM. Principles and Practice of Sleep Medicine (Fourth Edition). *Part Princ Sleep Medicine Sect 2sleep Mech Sect 2 Sleep Mech*. Published online 2005:120-135. doi:10.1016/b0-72-160797-7/50017-3

53. Ramot M, Fisch L, Davidesco I, et al. Emergence of Sensory Patterns during Sleep Highlights Differential Dynamics of REM and Non-REM Sleep Stages. *J Neurosci*. 2013;33(37):14715-14728. doi:10.1523/jneurosci.0232-13.2013

54. Thomson DJ. Spectrum estimation and harmonic analysis. *P Ieee*. 1982;70(9):1055-1096. doi:10.1109/proc.1982.12433

55. Slepian D. On bandwidth. *P Ieee*. 1976;64(3):292-300. doi:10.1109/proc.1976.10110

56. Slepian D. Prolate spheroidal wave functions, fourier analysis, and uncertainty — V: the discrete case. *Bell Syst Technical J*. 1978;57(5):1371-1430. doi:10.1002/j.1538-7305.1978.tb02104.x

57. Lepage KQ, Fleming CN, Witcher M, Vijayan S. Multitaper estimates of phase-amplitude coupling. *J Neural Eng*. 2021;18(5):056028. doi:10.1088/1741-2552/ac1deb

58. Bokil H, Andrews P, Kulkarni JE, Mehta S, Mitra PP. Chronux: A platform for analyzing neural signals. *J Neurosci Meth*. 2010;192(1):146-151. doi:10.1016/j.jneumeth.2010.06.020

59. Vijayan S, Lepage KQ, Kopell NJ, Cash SS. Frontal beta-theta network during REM sleep. *Elife*. 2017;6:e18894. doi:10.7554/elife.18894

60. Andrillon T, Nir Y, Cirelli C, Tononi G, Fried I. Single-neuron activity and eye movements during human REM sleep and awake vision. *Nat Commun*. 2015;6(1):7884. doi:10.1038/ncomms8884

61. Staresina BP, Bergmann TO, Bonnefond M, et al. Hierarchical nesting of slow oscillations, spindles and ripples in the human hippocampus during sleep. *Nat Neurosci*. 2015;18(11):1679-1686. doi:10.1038/nn.4119

62. Simor P, Gombos F, Blaskovich B, Bódizs R. Long-range alpha and beta and short-range gamma EEG synchronization distinguishes phasic and tonic REM periods. *Sleep*. 2017;41(3). doi:10.1093/sleep/zsx210

63. Benca RM, Obermeyer WH, Larson CL, et al. EEG alpha power and alpha power asymmetry in sleep and wakefulness. *Psychophysiology*. 1999;36(4):430-436. doi:10.1111/1469-8986.3640430

64. Carli FD, Proserpio P, Morrone E, et al. Activation of the motor cortex during phasic rapid eye movement sleep. *Ann Neurol*. 2016;79(2):326-330. doi:10.1002/ana.24556

65. Simor P, Wijk G van der, Nobili L, Peigneux P. The microstructure of REM sleep: why phasic and tonic? *Sleep Med Rev*. 2020;52:101305. doi:10.1016/j.smrv.2020.101305

66. Cantero JL, Atienza M, Stickgold R, Kahana MJ, Madsen JR, Kocsis B. Sleep-dependent theta oscillations in the human hippocampus and neocortex. *J Neurosci Official J Soc Neurosci*. 2003;23(34):10897-10903.

67. Nishida M, Uchida S, Hirai N, et al. High frequency activities in the human orbitofrontal cortex in sleep–wake cycle. *Neurosci Lett*. 2005;379(2):110-115. doi:10.1016/j.neulet.2004.12.069

68. Cox R, Rüber T, Staresina BP, Fell J. Phase-based coordination of hippocampal and neocortical oscillations during human sleep. *Commun Biology*. 2020;3(1):176. doi:10.1038/s42003-020-0913-5

69. Frauscher B, Ellenrieder N von, Dolezalova I, Bouhadoun S, Gotman J, Peter-Derex L. REM sleep sawtooth waves are associated with widespread cortical activations. *J Neurosci*. Published online 2020:JN-RM-1586-20. doi:10.1523/jneurosci.1586-20.2020

70. Corsi-Cabrera M, Velasco F, Río-Portilla Y del, et al. Human amygdala activation during rapid eye movements of rapid eye movement sleep: an intracranial study. *J Sleep Res*. 2016;25(5):576-582. doi:10.1111/jsr.12415

71. Axmacher N, Elger CE, Fell J. Ripples in the medial temporal lobe are relevant for human memory consolidation. *Brain*. 2008;131(7):1806-1817. doi:10.1093/brain/awn103

72. Ji D, Wilson MA. Coordinated memory replay in the visual cortex and hippocampus during sleep. *Nat Neurosci*. 2007;10(1):100-107. doi:10.1038/nn1825

73. Skaggs WE, McNaughton BL. Replay of Neuronal Firing Sequences in Rat Hippocampus During Sleep Following Spatial Experience. *Science*. 1996;271(5257):1870-1873. doi:10.1126/science.271.5257.1870

74. Wilson MA, McNaughton BL. Reactivation of Hippocampal Ensemble Memories During Sleep. *Science*. 1994;265(5172):676-679. doi:10.1126/science.8036517

75. Siapas AG, Wilson MA. Coordinated Interactions between Hippocampal Ripples and Cortical Spindles during Slow-Wave Sleep. *Neuron*. 1998;21(5):1123-1128. doi:10.1016/s0896-6273(00)80629-7

76. Lee AK, Wilson MA. Memory of Sequential Experience in the Hippocampus during Slow Wave Sleep. *Neuron*. 2002;36(6):1183-1194. doi:10.1016/s0896-6273(02)01096-6

77. Sirota A, Csicsvari J, Buhl D, Buzsáki G. Communication between neocortex and hippocampus during sleep in rodents. *Proc National Acad Sci*. 2003;100(4):2065-2069. doi:10.1073/pnas.0437938100

78. Cox R, Rüber T, Staresina BP, Fell J. Heterogeneous profiles of coupled sleep oscillations in human hippocampus. *Neuroimage*. 2019;202:116178. doi:10.1016/j.neuroimage.2019.116178

79. Piantoni G, Halgren E, Cash SS. Spatiotemporal characteristics of sleep spindles depend on cortical location. *Neuroimage*. 2017;146:236-245. doi:10.1016/j.neuroimage.2016.11.010

80. Cox R, Mylonas DS, Manoach DS, Stickgold R. Large-scale structure and individual fingerprints of locally coupled sleep oscillations. *Sleep*. 2018;41(12). doi:10.1093/sleep/zsy175

81. Cox R, Hofman WF, Boer M de, Talamini LM. Local sleep spindle modulations in relation to specific memory cues. *Neuroimage*. 2014;99:103-110. doi:10.1016/j.neuroimage.2014.05.028

82. Salmelin R, Hari R. Spatiotemporal characteristics of sensorimotor neuromagnetic rhythms related to thumb movement. *Neuroscience*. 1994;60(2):537-550. doi:10.1016/0306-4522(94)90263-1

83. Tiihonen J, Hari R, Kajola M, Karhu J, Ahlfors S, Tissari S. Magnetoencephalographic 10-Hz rhythm from the human auditory cortex. *Neurosci Lett*. 1991;129(2):303-305. doi:10.1016/0304-3940(91)90486-d

84. Saalmann YB, Pinsk MA, Wang L, Li X, Kastner S. The Pulvinar Regulates Information Transmission Between Cortical Areas Based on Attention Demands. *Science*. 2012;337(6095):753-756. doi:10.1126/science.1223082

85. Jensen O, Gelfand J, Kounios J, Lisman JE. Oscillations in the Alpha Band (9–12 Hz) Increase with Memory Load during Retention in a Short-term Memory Task. *Cereb Cortex*. 2002;12(8):877-882. doi:10.1093/cercor/12.8.877

86. Vijayan S, Kopell NJ. Thalamic model of awake alpha oscillations and implications for stimulus processing. *P Natl Acad Sci Usa*. 2012;109(45):18553-18558. doi:10.1073/pnas.1215385109

87. Lobier M, Palva JM, Palva S. High-alpha band synchronization across frontal, parietal and visual cortex mediates behavioral and neuronal effects of visuospatial attention. *Neuroimage*. 2018;165:222-237. doi:10.1016/j.neuroimage.2017.10.044

88. Palva S, Kulashekhar S, Hämäläinen M, Palva JM. Localization of Cortical Phase and Amplitude Dynamics during Visual Working Memory Encoding and Retention. *J Neurosci*. 2011;31(13):5013-5025. doi:10.1523/jneurosci.5592-10.2011

89. Stein A von, Chiang C, König P. Top-down processing mediated by interareal synchronization. *Proc National Acad Sci*. 2000;97(26):14748-14753. doi:10.1073/pnas.97.26.14748

90. Palva JM, Palva S, Kaila K. Phase Synchrony among Neuronal Oscillations in the Human Cortex. *J Neurosci*. 2005;25(15):3962-3972. doi:10.1523/jneurosci.4250-04.2005

91. Vijayan S, Ching S, Purdon PL, Brown EN, Kopell NJ. Thalamocortical Mechanisms for the Anteriorization of Alpha Rhythms during Propofol-Induced Unconsciousness. *J Neurosci*. 2013;33(27):11070-11075. doi:10.1523/jneurosci.5670-12.2013

92. Palva S, Palva JM. New vistas for α-frequency band oscillations. *Trends Neurosci*. 2007;30(4):150-158. doi:10.1016/j.tins.2007.02.001

93. Danker-Hopfe H, Anderer P, Zeitlhofer J, et al. Interrater reliability for sleep scoring according to the Rechtschaffen & Kales and the new AASM standard. *J Sleep Res*. 2009;18(1):74-84. doi:10.1111/j.1365-2869.2008.00700.x

94. Cerioli A. K-means cluster analysis and Mahalanobis metrics: a problematic match or an overlooked opportunity. *Statistica Applicata*. 2005;17(1):61–73.

95. Martino A, Ghiglietti A, Ieva F, Paganoni AM. A k-means procedure based on a Mahalanobis type distance for clustering multivariate functional data. *Statistical Methods Appl*. 2019;28(2):301-322. doi:10.1007/s10260-018-00446-6

96. Faber V. Clustering and the continuous k-means algorithm. *Los Alamos Science*. 1994;67.

97. Akaike H. A new look at the statistical model identification. *Ieee T Automat Contr*. 1974;19(6):716-723. doi:10.1109/tac.1974.1100705

98. deLeeuw J. Breakthroughs in Statistics, Foundations and Basic Theory. *Springer Ser Statistics*. Published online 1992:599-609. doi:10.1007/978-1-4612-0919-5_37

99. Cavanaugh JE, Shumway RH. An Akaike information criterion for model selection in the presence of incomplete data. *J Stat Plan Infer*. 1998;67(1):45-65. doi:10.1016/s0378-3758(97)00115-8

100. Dempster AP, Laird NM, Rubin DB. Maximum Likelihood from Incomplete Data Via the EM Algorithm. *J Royal Statistical Soc Ser B Methodol*. 1977;39(1):1-22. doi:10.1111/j.2517-6161.1977.tb01600.x